

American Journal of Science

SUMMER 1995

THE PALEOZOIC WORLD: CONTINENTAL FLOODING, HYPSOMETRY, AND SEALEVEL

THOMAS J. ALGEO* and KIRILL B. SESLAVINSKY**

ABSTRACT. Comparative analysis of multiple paleocontinental flooding records permits partial reconstruction of continental and global hypsometries, calculation of continental and global sealevel elevation trends, and isolation of elevation residuals that may record secular changes in hypsometry, for example, as a result of continental epeirogeny. Analysis of the flooding records of 13 Paleozoic landmasses suggests that the mid-Ordovician eustatic maximum was about 100 to 225 m above present sealevel, substantially lower than previous estimates of +300 m (Vail, Mitchum, and Thompson, 1977) to +600 m (Hallam, 1984) and closer to estimates of 175 to 250 m above present sealevel for the mid-Cretaceous eustatic maximum.

The most important control on Paleozoic elevation estimates is choice of a modern hypsometric analog for scaling of paleo-hypsometries: an American analog yields elevations that are about 100 m higher than a Eurasian analog. Differences in the elevation scales between analogs result in dissimilar global hypsometries: relative to the modern world, a Eurasian analog yields gentle Cambro-Carboniferous and intermediate Permian hypsometries, whereas an American analog yields intermediate Cambro-Carboniferous and steep Permian hypsometries. These observations have important but unexplored implications for relationships between global tectonics, continental geomorphology, and eustasy.

Variance in paleocontinental flooding records includes contributions from hypsometric, eustatic, and residual sources. Differences in the time-averaged mean hypsometry of paleocontinents account for the largest proportion of flooding variance (95 percent). Because continental hypsometry is closely linked to landmass area, corrections for variable landmass area are necessary in all hypsometric analyses of flooding records. Of the 5 percent of variance of non-hypsometric origin, eustatic factors account for only one fifth overall but from one to two thirds for paleocontinents with high-quality flooding records. The Paleozoic continents yielding the best records of eustasy are Baltica, North China/United China, Kazakhstania, and Siberia; Laurentia/Laurussia, although having a high-quality flooding record, exhibits almost no eustatic component to variance, making its use as a global standard questionable.

* H. N. Fisk Laboratory of Sedimentology, Department of Geology, University of Cincinnati, Cincinnati, Ohio 45221-0013.

** Institute of Physics of the Earth, B. Gruzinskaya 10, 123810 Moscow, Russia.

INTRODUCTION

Paleozoic Eustasy

An accurate record of secular changes in global sealevel elevation is important for understanding a wide range of geologic processes that either contribute to or respond to such variation, for example, mantle convection and heatflow (Gurnis, 1990; Galer, 1991), geotectonic/climatic cycles (Fischer, 1984; Worsley, Nance, and Moody, 1984), atmospheric CO₂ levels and carbonate equilibria (Wilkinson, Owen, and Carroll, 1985; Wilkinson and Given, 1986), sediment fractionation and mass cycling (Davies and Worsley, 1981; Wilkinson and Walker, 1989), the global water cycle (Tardy, N'Koukou, and Probst, 1989), evaporite deposition (Railsback, 1992), and biodiversity (Riding, 1984). Such a record would assist in investigation of links between mantle/tectonic processes, atmospheric/oceanic chemistry, and sediment/geochemical fluxes and could serve as a proxy for other, more poorly known variables in global models.

Despite the obvious importance of and need for accurate eustatic records, surprisingly little research has been undertaken on long-term global sealevel changes. To date, the only widely-cited studies are those of Vail, Mitchum, and Thompson (1977) and Hallam (1984), and, although each of these was a major pioneering effort in eustatic analysis, the resulting sealevel curves may be seriously flawed. The Vail, Mitchum, and Thompson curve is ostensibly based on seismic stratigraphy, but the Paleozoic portion, for which supporting data have never been published, bears a strong resemblance to the North American cratonic sequences of Sloss (1963; compare Miall, 1986). The Hallam curve is based on hypsometric analysis and combines area-elevation data for modern continents (Kossinna, 1933) with flooding data from paleogeographic atlases of the USSR (Vinogradov, 1967-1969) and North America (Schuchert, 1955; see Hallam, 1977). This technique resulted in sealevel estimates up to 600 m above present sealevel, but all Paleozoic eustatic elevations are too high owing to use of inappropriate hypsometric models. Because small land-masses have gentler area-elevation distributions than large ones, combining flooding data from small paleocontinents (for example, Paleozoic cratons within the USSR) with hypsometric curves for large modern continents (for example, Eurasia) results in systematic overestimation of sealevel elevations (Algeo and Wilkinson, 1991).

The Hallam study illustrates a major problem in hypsometric analysis of eustasy, that is, selection of an appropriate area-elevation model with which to transform ancient flooding records to sealevel elevations. Because paleocontinental hypsometries cannot be reconstructed on purely theoretical grounds, modern continental hypsometries must be used as analogs. The fundamental difficulty with this approach is that continental area-elevation distributions change through time in response to geotectonic events (for example, continental rifting or collision) and tectonic evolution of continental margins (for example, passive to active). Consequently, a given modern hypsometric curve is likely to yield increasingly

less accurate sealevel estimates for progressively older epochs. This limitation has largely constrained hypsometric studies of eustasy to the Cretaceous and younger (for example, Bond, 1976, 1978a, 1978b, 1979; Harrison and others, 1981, 1983; Veevers, 1984), and, in the absence of quantitative hypsometric analysis, existing Paleozoic sealevel curves are mostly qualitative reconstructions based on sequence stratigraphic interpretations (Dennison and Head, 1975; Johnson, Klapper, and Sandberg, 1985; Heckel, 1986; Ross and Ross, 1988; Johnson, Kaljo, and Rong, 1991). Herein, we develop a new method of reconstructing paleocontinental hypsometries based on comparative analysis of flooding records from multiple co-existing landmasses and utilize these area-elevation reconstructions to calculate Paleozoic eustatic elevations.

Continental Hypsometry

The hypsometry of a topographic surface is its cumulative areal frequency with respect to elevation. Continental area-elevation distributions form sigmoidal curves that are convex up at low elevations, concave up at high elevations, and have an inflection point close to sealevel (fig. 1). The rate of change of elevation with respect to cumulative area is termed "hypsometric slope" and is a measure of the rate of potential flooding of a landmass within a given elevation range (Algeo and Wilkinson, 1991). The inflection point is the elevation at which the slope of the curve is gentlest and, thus, at which a landmass is potentially most rapidly floodable. The sigmoidal shape of continental hypsometric curves is probably controlled by a balance between net continent-interior erosion and net continent-margin deposition. For epeirogenically stable landmasses, the inflection point coincides approximately with the boundary between erosional and depositional regimes, usually at the updip margin of coastal-plain wedges at an elevation of several tens of meters above sealevel.

Hypsometric curves can be used to convert flooding data to sealevel elevations, and secular changes in sealevel elevation can be reconstructed from a series of paleogeographic maps (fig. 1A–C). Because Phanerozoic sealevel fluctuations are limited to an elevation range within a few hundred meters of present sealevel (Vail, Mitchum, and Thompson, 1977; Worsley, Nance, and Moody, 1984), only the low-elevation portion of a hypsometric curve ("coastal hypsometry") is of significance for eustatic studies. Within this elevation range, flooding data provide information about the area-elevation characteristics of a landmass that can be used partially to reconstruct coastal hypsometries. We term reconstructed linear segments of paleocontinental area-elevation distributions "hypsometric chords" (fig. 1D).

The hypsometric method offers several advantages for reconstruction of long-term eustatic trends (Hallam, 1992). Integration of flooding data over large, relatively stable cratonic areas avoids difficulties arising in seismic stratigraphic studies from convolution of eustasy with passive margin subsidence (Pitman, 1978). Although the hypsometric method

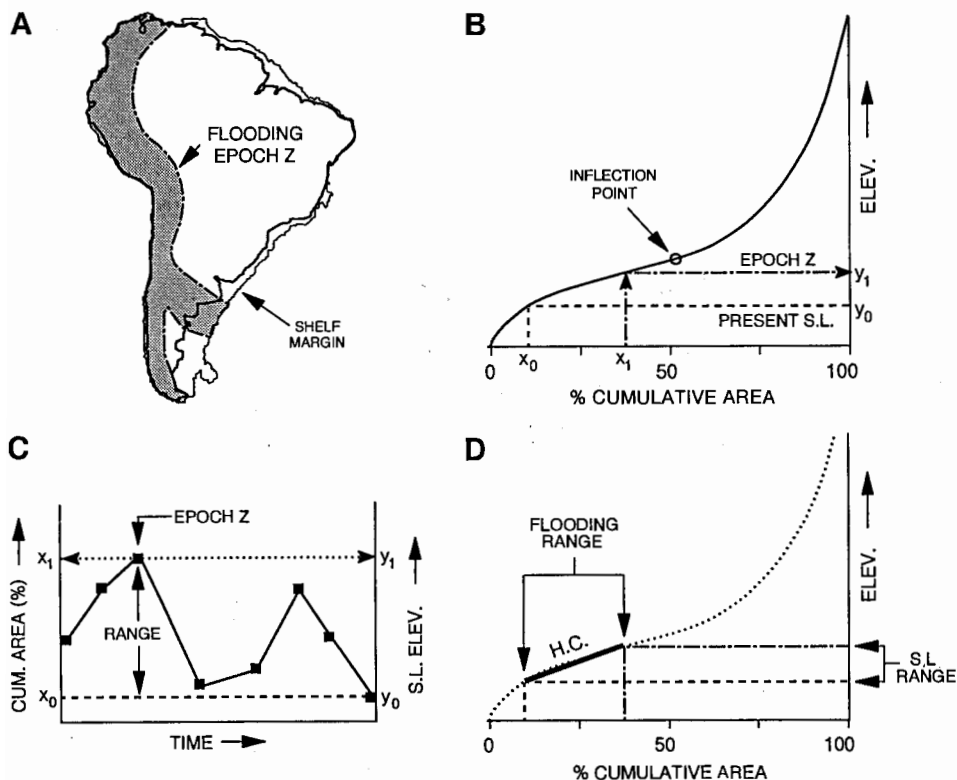


Fig. 1. Example of calculation of sealevel elevations using hypsometry and continental flooding data. (A) Area flooded for a given epoch is measured from an equal-area paleogeographic map relative to a specified reference level, such as the shelf margin. (B) Fractional area flooded (x_1) is converted to sealevel elevation (y_1) using a landmass-specific hypsometric curve. (C) Secular sealevel elevation curve is constructed from a series of paleogeographic maps. (D) Given time-invariant continental coastal hypsometry, a specified flooding range yields a corresponding range of sealevel elevations. A "hypsometric chord" (H.C.) is a linear representation of part of a continental area-elevation distribution.

does not yield as high a temporal resolution as seismic or sequence stratigraphic analysis owing to use of relatively coarse time slices, it is probably superior for estimating absolute eustatic elevations. Furthermore, the technique is applicable to the entire Phanerozoic, unlike mid-ocean ridge volume analysis (Pitman, 1978; Kominz, 1984).

PALEOZOIC HYPOMETRIC-SEALEVEL ANALYSIS

Continental flooding, hypsometry, and eustasy are interrelated such that, given knowledge regarding the time-dependent status of two of these variables, it is possible to solve for the third (fig. 1). In practice, fairly reliable information exists only with respect to paleocontinental flooding, and it is necessary to estimate one of the remaining parameters

(for example, hypsometry) in order to arrive at the other (for example, eustasy). We have developed a method of partially reconstructing paleocontinental hypsometries based on the premises that: (1) comparative analysis of multiple flooding records permits isolation of a component of variance common to all continents and one unique to each continent, (2) these components represent eustasy and time-averaged coastal hypsometry, respectively, and (3) modern continents in "hypsometric equilibrium" are representative of continental area-elevation relations throughout the Phanerozoic and, therefore, can be used to scale both paleocontinental hypsometries and eustatic elevations.

Paleozoic Continental Flooding

Paleogeographic database.—Our comparative analysis is based on the Paleozoic flooding records of thirteen landmasses: Pangea, Gondwana, Laurussia, Laurentia, Baltica, Armorica, Siberia, Kazakhstania, North China, South China, United China, Indochina, and Chukotka. Flooding data for these paleocontinents were assembled in two stages. In the first stage, lithologic and tectonic data were compiled for 18 Proterozoic and Paleozoic time slices for each of six continents in modern coordinates (fig. 2). These data were plotted on 108 polyconic base maps at a 1:25,000,000 scale and published as 18 global maps at a 1:60,000,000 scale in Ronov, Khain, and Seslavinsky (1984). In the second stage, lithologic data were transferred to the global paleogeographic reconstructions of Scotese and others (1979), and areas of paleo-flooding were interpreted based on the distribution of preserved marine and continental strata of a given age. These paleogeographic reconstructions were published as 7 Mercator projection maps at a 1:120,000,000 scale in Ronov, Khain, and Seslavinsky (1984) and subsequently converted to equal-area projections for calculation of total landmass and flooded areas. Methods of compilation of the original database were discussed in Ronov, Migdisov, and Khain (1972), Ronov, Khain, and Seslavinsky (1976), and Ronov and others (1980).

The base maps and paleogeographic reconstructions have been updated since initial publication using new sources, including Wang (1985), the Paleogeographic Atlas of Australia (1988, 1992), and Ziegler (1989), among others. These data have been replotted on a new generation of paleogeographic reconstructions (Zonenshain, Kuzmin, and Kononov, 1987; Zonenshain, Kuzmin, and Natapov, 1990) with modifications from other sources (Scotese and McKerrow, 1990; Nie, Rowley, and Ziegler, 1990; Robardet, Paris, and Racheboeuf, 1990; Torsvik and others, 1991). The new paleogeographic maps were published in Khain and Seslavinsky (1991), and Seslavinsky (1987, 1991) provides further discussion of compilation methods. Both sets of maps are under continuous revision, and new editions are in preparation for publication (Seslavinsky).

Certain technical problems arise in using paleogeographic data as a record of secular changes in continental flooding. First, data collection

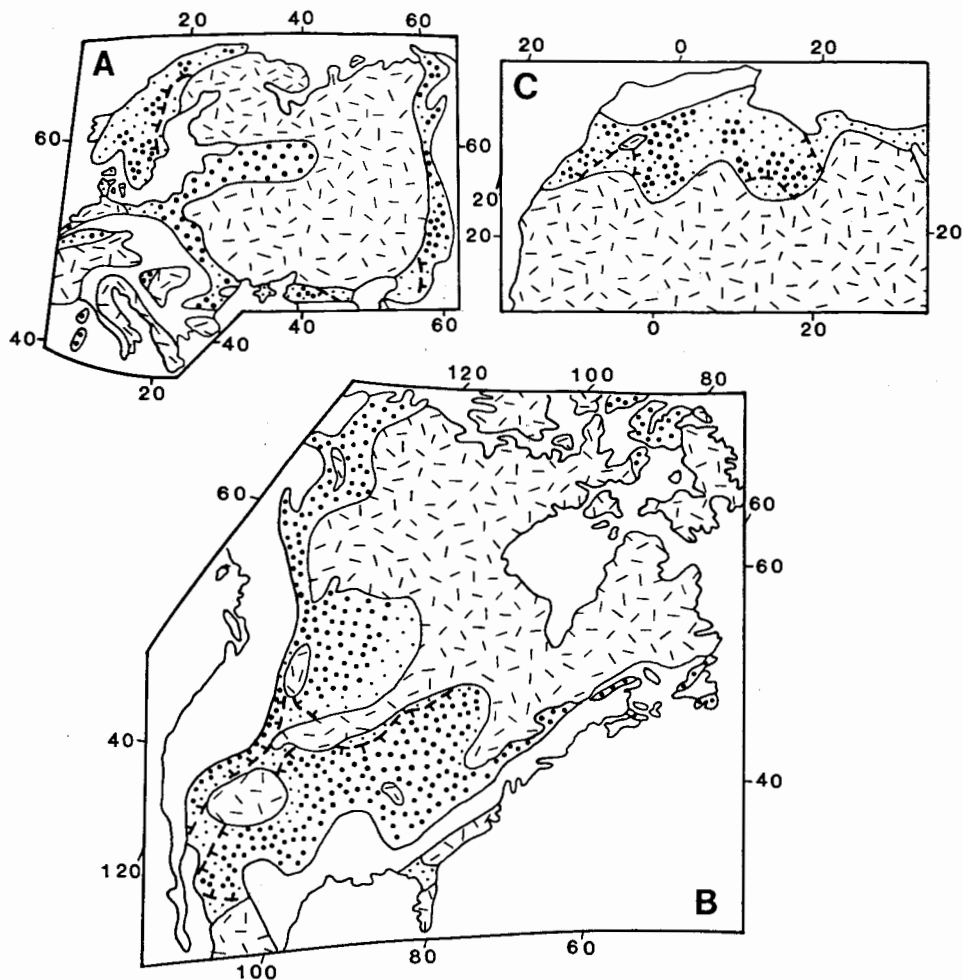


Fig. 2. Examples of paleocontinental flooding data: the Early Ordovician (Tremadoc-Arenig, Canadian) of the Eastern European (A), North American (B), and North African (C) platforms. Random dashes = land areas, large dots = area of extant Lower Ordovician marine strata, small dots = interpretative reconstruction of areas of probable Early Ordovician flooding, unpatterned areas = mobile belts or younger terranes. Flooding estimates: $F(ij)_{\min}$ = large and small dots within heavy dashed lines; $F(ij)_{\text{mean}}$ = all dotted areas; $F(ij)_{\max}$ not shown. Paleogeographic reconstructions shown in A, B, and C have quality ratings of excellent, good, and fair, respectively. These panels are excerpts from the 1:25,000,000 lithologic base maps used in preparation of the Paleozoic paleogeographic atlas of Ronov, Khain, and Sestlavinsky (1984).

must be constrained to specific tectonic elements. The Paleozoic lithologic basemaps include four continental tectonic subdivisions: cratons, platforms, geosynclines, and orogens (Ronov, Khain, and Sestlavinsky, 1984). In this study, flooding was calculated for cratons and platforms

alone; geosynclines are deep-water basins underlain in part by oceanic crust (Ronov, Khain, and Sestlavinsky, 1984), and the complex tectonic structure of many geosynclines and orogens makes palinspastic reconstruction and areal estimation difficult for these regions. Second, Paleozoic stratigraphic data are unavailable from many modern continental shelves, and data generation was largely constrained to present emergent continental areas. Third, secular changes in the size of continents (both individually and collectively; for example, Sestlavinsky, 1986) necessitate evaluation of secular changes in continental flooding as a fractional rather than an absolute area (Ronov and others, 1980; compare Ronov, 1994). Fourth, because paleogeographic data are generally compiled for time intervals of finite duration, the apportionment of time is important. Paleogeographic maps comprising progressively longer time slices integrate flooding over more numerous discrete transgressive-regressive episodes, thereby tending to exaggerate flooding with respect to any one moment in time (Wise, 1974). We have attempted to minimize this problem by dividing each Paleozoic period into two or three time slices of sub-equal duration (informally termed "epochs"), yielding 15 intervals representing from 9 to 40 my and averaging 22 my. We use the timescale of Harland and others (1990), modified according to Bowring and others (1993) and Landing (1994). Fifth, uncertainties regarding the original extent of marine strata on continents result from loss of sediments through erosion, metamorphism, and deep burial. Continental sediments are relatively long-lived, however, exhibiting exponential survivorship with a half-life of about 130 my (Gregor, 1985) to 380 my (Wilkinson and Walker, 1989). The expected lower survivorship of progressively older marine strata has been compensated for through somewhat greater extrapolative reconstruction of Early Paleozoic flooded areas, manifested in broader uncertainty limits for some continents (fig. 3). In working exclusively within the Paleozoic, we hope to obviate problems associated with large first-order differences in sediment survivorship patterns between the Paleozoic and Mesozoic-Cenozoic geotectonic cycles (Ronov, 1994).

Flooding estimates.—For each Paleozoic continent, absolute estimates of total landmass and flooded areas were determined by epoch (fig. 3). Fractional flooding of continent i at epoch j is defined as the flooded area divided by total landmass area, for which minimum, mean, and maximum values were estimated, $F(ij)_{\min}$, $F(ij)_{\text{mean}}$, and $F(ij)_{\max}$ (table 1). Minimum flooding values are based on areas of preserved marine strata of a given age extrapolated slightly to link erosional outliers to the contemporaneous global ocean (fig. 2). Mean or "most likely" flooding values are based on more extensive restoration of flooded areas to account for loss of marine strata owing to subsequent regional uplift and erosion; such restoration was guided by facies and isopach trends of extant strata of a given age (see Khain and Sestlavinsky, 1991, for discussion of techniques of paleogeographic reconstruction). Estimation of maximum possible flooding values is more difficult owing to the need for greater extrapolation beyond available stratigraphic data. For ease of

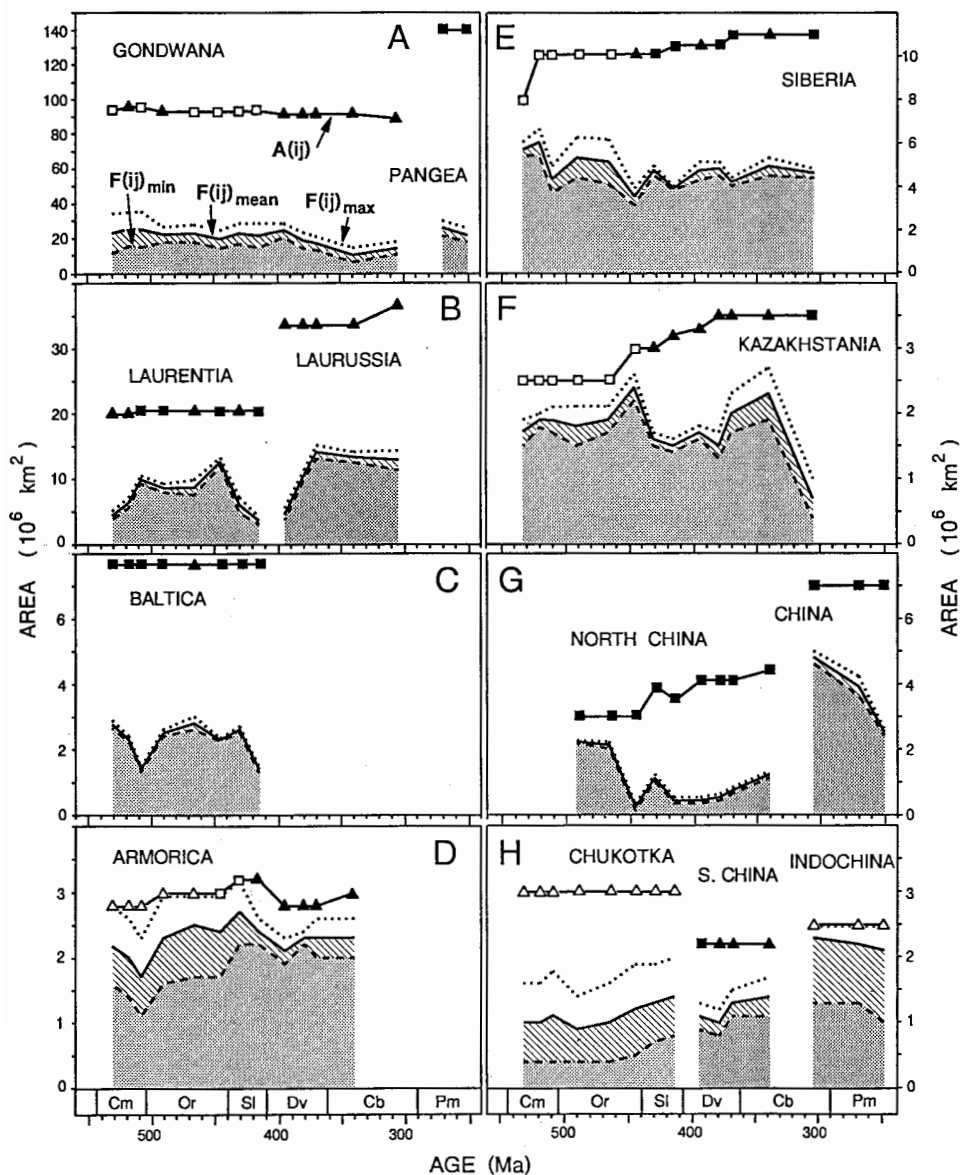


Fig. 3. Flooding data for 13 Paleozoic continents of this study. Shown are estimates of total landmass area ($A(ij)$; upper solid line), minimum flooding ($F(ij)_{min}$; dashed line), mean or "most-likely" flooding ($F(ij)_{mean}$; lower solid line), and maximum flooding ($F(ij)_{max}$; dotted line). Stratigraphic data quality indicated by symbols at top: excellent (solid squares), good (solid triangles), fair (open squares), or poor (open triangles). All data are plotted versus age midpoints for Paleozoic 15 "epochs": Early/Middle/Late Cambrian, E/M/L Ordovician, E/L Silurian, E/M/L Devonian, E/L Carboniferous, and E/L Permian. Sources of data are cited in text.

TABLE 1
*Paleozoic flooding data by continent and epoch**

epoch	age [†]	GOND	PNG	LRNT	LRSS	BALT	SIB	ARM	CHK	KAZ	N-CHN	U-CHN	S-CHN	IND
LPM	250		15.8									35.7		84.0
EPM	270		18.7									55.7		88.0
LCB	305	16.8			34.6		41.8	76.6		20.0		68.5		92.0
ECB	340	12.0			39.4		44.5			65.7	27.2		63.6	
LDV	370	19.4			41.7		38.1	82.1		57.1	17.0		59.0	
MDV	380	21.1			31.3		45.7	82.1		42.8	12.1		45.4	
EDV	395	27.6			13.4		44.7	75.0		51.5	9.7		50.0	
LSL	415	23.7		17.0		18.1	37.1	75.0	46.6	46.8	11.4			
ESL	430	25.1		28.7		33.7	46.5	84.3	43.3	53.3	28.2			
LOR	445	21.7		60.9		29.8	34.6	80.0	40.0	80.0	6.6			
MOR	465	25.1		41.9		36.3	50.4	83.3	33.3	76.0	70.0			
EOR	490	24.5		41.4		32.4	52.4	76.6	30.0	72.0	73.3			
LCM	510	26.9		47.8		18.1	42.5	60.7	36.6	76.0				
MCM	515	27.2		31.0		29.8	59.4	71.4	33.3	76.0				
ECM	525	24.7		21.0		36.3	72.1	78.5	33.3	68.0				

* Fractional flooding of total landmass area in percent for mean case, $F(i)_{\text{mean}}$. Estimates based on interpretative paleogeographic maps of Khain and Sesslavinsky (1991).

[†] Ages of epoch midpoints in Ma.

TABLE 2
Flooding ranges for Paleozoic continents*

	Mean	Minimum	Maximum
Gondwana	22.8±4.3	16.3±3.8	29.3±6.1
Pangea	17.3±1.4	14.3±1.2	20.3±1.7
Laurentia	36.2±13.6	32.4±13.9	40.1±13.5
Laurussia	32.1±10.0	29.2±10.0	35.0±10.1
Baltica	29.3±6.8	28.0±6.7	30.8±7.0
Siberia	46.9±9.6	42.7±9.0	51.2±10.9
Armorica	77.1±6.2	61.3±10.5	92.0±7.6
Chukotka	37.0±5.3	16.7±5.0	57.5±6.4
Kazakstania	60.4±16.6	53.5±16.3	67.4±17.5
North China	28.4±24.1	25.8±24.3	31.0±24.0
United China	53.3±13.5	50.5±12.8	56.2±14.3
South China	54.5±7.1	44.3±5.9	64.8±8.7
Indochina	88.0±3.2	48.0±5.7	100.0±0.0

* Fractional flooding of total landmass area in percent. Flooding ranges, that is, $\mu_F(i) \pm \sigma_F(i)$, represent mean Paleozoic flooding plus or minus one standard deviation calculated from mean, minimum, and maximum flooding values, $F(ij)_{\text{mean}}$, $F(ij)_{\text{min}}$ and $F(ij)_{\text{max}}$.

Ages of epoch midpoints in Ma.

computation, we calculate a maximum value based on the assumption that the maximum area of marine strata lost to erosion is no greater than twice that of our most-likely case:

$$F(ij)_{\text{max}} = 2 \cdot F(ij)_{\text{mean}} - F(ij)_{\text{min}} \quad (1)$$

For each continent, mean flooding for the Paleozoic as a whole is calculated as an unweighted average of epochal flooding estimates:

$$\mu_F(i) = j \sum_1^n F(ij)/n \quad (2)$$

where $\mu_F(i)$ is mean flooding of continent i , $F(ij)$ is the flooding value of choice for continent i at epoch j , and n is the number of epochs during which continent i was an independent entity. The range of Paleozoic flooding for continent i is:

$$r_F(i) = \mu_F(i) \pm \sigma_F(i) \quad (3)$$

$$\sigma_F(i) = \left[j \sum_1^n [F(ij) - \mu_F(i)]^2 / n \right]^{0.5} \quad (4)$$

where $r_F(i)$ is range of flooding of continent i , and $\sigma_F(i)$ is the standard deviation of flooding values of continent i (table 2). As true range is often a poor measure of variance in a dataset, we use the standard deviation range (that is, plus or minus one standard deviation about the mean).

The reliability of paleocontinental flooding estimates is a function of accuracy of the lithologic basemaps, soundness of paleogeographic interpretations, and precision of measurement. The completeness and quality of stratigraphic data available for basemap construction varies by continent and epoch and is assessed using a semi-quantitative scale (excellent, good, fair, poor; fig. 3). Uncertainties in paleogeographic interpretations are accounted for through use of minimum, mean, and maximum flooding estimates (fig. 3; table 2). Average intra-epochal uncertainty in continental flooding values, $F(ij)_{\text{mean}} \pm F(ij)_{\text{min/max}}$, ranges from ± 5 percent for Baltica and United China to ± 55 percent for Chukotka, whereas average interepochal variation in flooding values, that is, $\pm 1 \sigma F(i)_{\text{mean}}$, ranges from ± 4 percent for Indochina to ± 85 percent for North China (table 3). When inter-epochal variability exceeds intra-epochal uncertainty, flooding data are generally more reliable and secular trends in resultant sealevel elevation estimates are more likely to be significant. In this regard, Paleozoic continents yielding relatively reliable trends include Laurentia, Laurussia, Baltica, Siberia, Kazakhstania, North China, and United China, whereas those yielding rather unreliable trends include Armorica, Chukotka, and Indochina (table 3). Analytical precision in measurement of areas is ± 3 percent (Ronov, Migdisov, and Khain, 1972; Seslavinsky, 1987).

Reconstruction of Paleozoic Continental Hypsometries

Assumptions.—Analysis of paleo-hypsometry and -eustasy using continental flooding records is based on certain fundamental assumptions.

TABLE 3
*Reliability of Paleozoic flooding trends**

	Intraepochal [#] uncertainty	Interepochal [†] variability
Gondwana	+28	+19
Pangea	+17	± 8
Laurentia	+10	+38
Laurussia	± 9	+31
Baltica	± 5	+23
Siberia	± 9	+20
Armorica	+20	± 8
Chukotka	+55	+14
Kazakhstan	+11	+27
North China	± 9	+85
United China	± 5	+25
South China	+19	+13
Indochina	+45	± 4

* Given as a percentage of mean Paleozoic flooding for each continent, $\mu F(i)_{\text{mean}}$.

[#] Average difference between mean and minimum or maximum flooding values, that is, $F(ij)_{\text{mean}} \pm F(ij)_{\text{min/max}}$.

[†] Standard deviation of Paleozoic flooding for mean case, that is, $\sigma F(i)_{\text{mean}}$.

Our method assumes that global sealevel elevations are uniform at any moment in time, and that changes in eustasy are globally synchronous. Although regional sealevel elevation anomalies exist in the modern world in the form of the geoid (Mörner, 1976), the spatial and temporal domains of geoidal variation are largely unknown and are assumed to average out to a global mean at epochal timescales. Any deviations of individual continental sealevel elevations from the global mean as a result of geoidal variations will appear as elevation residuals (below) and can be interpreted as such at that point. A corollary to the assumption of eustatic uniformity is that co-existing continents experienced the same mean, standard deviation and range of eustatic elevations for any given time interval (fig. 4A). Despite eustatic uniformity, differences in mean coastal hypsometry between coexisting landmasses result in different means and ranges of flooding values. Continents having stable long-term coastal hypsometries should exhibit a relatively narrow distribution of flooding values that mirrors the distribution of eustatic elevations, whereas those exhibiting "hypsometric instability" (that is, large epeirogenic motions) are likely to develop broader ranges of flooding values (fig. 4A).

Procedure.—Differences in flooding values between paleocontinents can be used partially to reconstruct a characteristic long-term mean hypsometry for each landmass (fig. 4A). Hypsometric reconstruction proceeds in two steps: (1) non-dimensional scaling of paleocontinental hypsometric chords, and (2) absolute scaling of hypsometric chords using a suitable modern hypsometric analog. In the first step, the means and ranges of flooding values for each paleocontinent are set equal to the same non-dimensional mean and range of eustatic elevations. Individual hypsometric chords are parameterized as:

$$'m(i) = 'r_s(w)/r_F(i) \quad (5)$$

$$'b(i) = '\mu_s(w) - 'm(i) \cdot \mu_F(i) \quad (6)$$

where $'m(i)$ and $'b(i)$ are non-dimensional estimates of hypsometric-chord slope and y-intercept for continent i , and $'\mu_s(w)$ and $'r_s(w)$ are non-dimensional values of the mean and range of global sealevel elevations (fig. 4A). This relative scaling procedure minimizes variance among resultant sealevel elevation estimates among continents and assigns as much of the total variance in flooding values as possible to differences in the time-averaged mean coastal hypsometries of continents. In the second step, dimensional values of the mean and range of eustatic elevations, $\mu_s(w)$ and $r_s(w)$, are substituted for $'\mu_s(w)$ and $'r_s(w)$, permitting calculation of dimensional values for the slopes and y-intercepts of paleocontinental hypsometric chords, $m(i)$ and $b(i)$. Dimensional values for the vertical elevation scale are determined from a modern continental analog (fig. 4B).

Choice of modern hypsometric analog.—A modern hypsometric analog must be used to scale paleo-elevation estimates, and, therefore, it is necessary to consider the hypsometric characteristics of modern land-

B

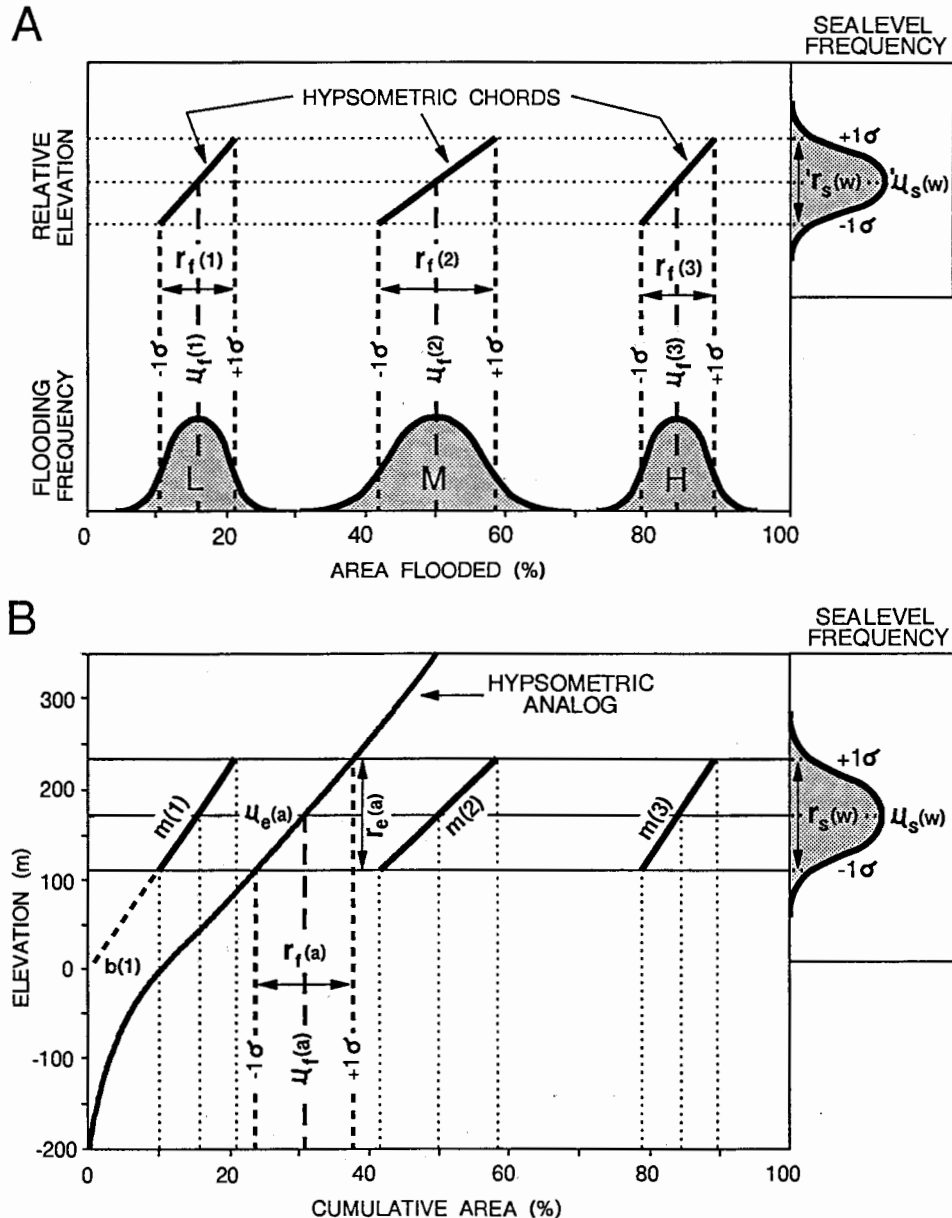


Fig. 4. Reconstruction of paleocontinental hypsometric chords. (A) Relative (non-dimensional) scaling of hypsometric chords for three coexisting landmasses exhibiting low (L), medium (M), and high (H) degrees of average flooding, $\mu_F(i)$, and variable flooding ranges, $\mu_F(i) \pm \sigma_F(i)$ (bottom). As coexisting landmasses experience the same mean and range of eustatic elevations (upper right), differences in means and ranges of flooding values among continents record differences in their coastal hypsometries (top). (B) Absolute scaling of hypsometric-chord elevations using a modern hypsometric analog, for which an "expected" range of flooding is estimated. Actual elevation range is dependent on choice of analog.

masses. The best available compilation of area-elevation data for modern continents is that of Harrison and others (1983), who utilized a Defense Mapping Agency database. This database contained global elevation values for 1 degree squares at latitudinal intervals of 100 m, offering a resolution superior to that of other extant databases. We have fitted the area-elevation data of Harrison and others (1983) with cubic splines to produce coastal hypsometric curves for the modern continents (fig. 5).

North America, South America, and Eurasia exhibit rather similar coastal hypsometries, having hypsometric slope minima of 5.0 to 6.7 m/percent area and inflection-point elevations slightly above present sea level (+15 m to +90 m; fig. 5). If the main control on the shape of continental hypsometries is the balance of continent-interior erosion and continent-margin deposition, these may represent equilibrium area-elevation distributions. On the other hand, the hypsometry of Africa exhibits an anomalously high inflection-point elevation (+310 m), and that of Australia exhibits two inflection points (−60 m and +110 m; fig.

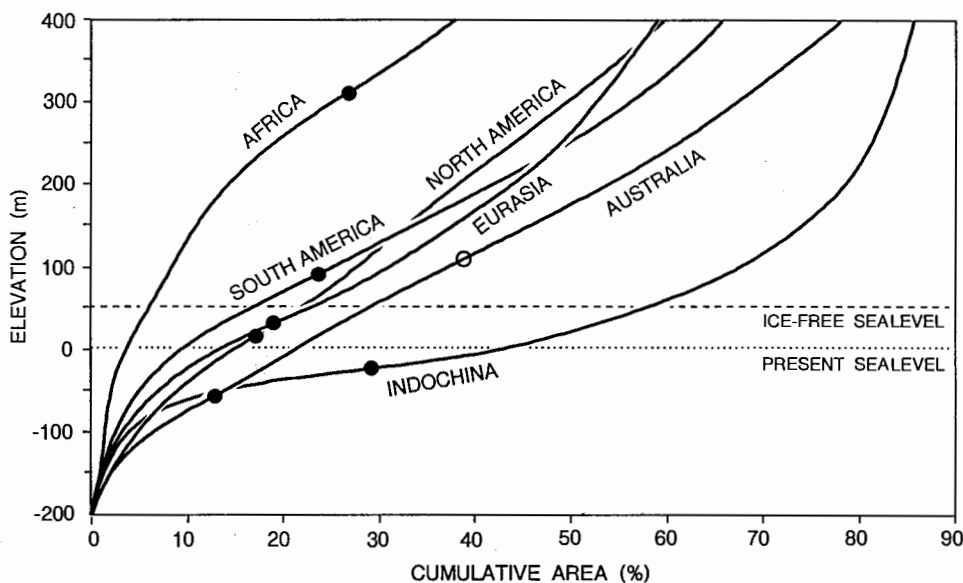


Fig. 5. Coastal hypsometries of modern continents (excluding Antarctica) with respect to shelf margins (about −200 m). Hypsometric curves are cubic-spline versions of the area-elevation data of Harrison and others (1983). The modern Indochina curve was calculated from equal-area 1:2,500,000 topographic maps and includes Borneo, Sumatra, Java, the Malaysian and Southeast Asian peninsulas (northward to the Song Ma-Red River region in northern Vietnam and westward to the Sagaing Fault zone in central Burma; Hutchison, 1989), and all intervening shallow-marine areas (≥ -200 m). Inflection points (in meters above sealevel, circles) and hypsometric-slope minima (in meters/percent area): Eurasia (+30; 5.0), Africa (+310; 6.7), North America (+15; 6.7), South America (+90; 5.6), Australia (−60 or +110; 5.6), and Indochina (−25; 1.4). Modern Indochina is included to illustrate the range of potential continental hypsometric variation.

5). Vertical adjustment of the African and Australian curves by -250 m and $+75$ m, respectively, would result in broad overlap of the coastal hypsometries of all five modern continents, suggesting that the anomalous character of the African and Australian curves may be a consequence of broad epeirogenic movements with amplitudes up to several hundred meters (Burke and Whiteman, 1973; Bond, 1978b; Smith, 1982; Sahagian, 1988; Sempéré and others, 1991). Probable recent large-scale epeirogenic motions of Africa and Australia suggest these continents may be in "hypsometric disequilibrium," rendering them unsuitable for use as hypsometric analogs. Therefore, in the following analysis, we utilize analogs based on the hypsometries of Eurasia and America (the latter an areally-weighted average of the coastal hypsometries of North and South America, which are similar in size and tectonic character).

The area-elevation curve of modern Indochina is shown not because it is a potential hypsometric analog, but because it illustrates the range of potential variation in continental hypsometries (fig. 5). Indochina has a subsea inflection-point elevation (-25 m) but exhibits no evidence of recent epeirogenic motion, suggesting that its hypsometry may represent an equilibrium condition associated with attenuated continental crust. This may be a common feature of tectonically independent small continents (that is, total area $< 10^7$ km²; Cogley, 1985) and may account for the high mean flooding values of many small Paleozoic landmasses.

Landmass area and flooding.—Landmass area is a major control on the steepness of a continent's coastal hypsometry and, thus, on its flooding record. Large continents are generally less "floodable" than small continents owing to a smaller ratio of low-elevation coastal area to total landmass area (Cogley, 1984, 1985; Algeo and Wilkinson, 1991). Consequently, for any given epoch, large continents tend to exhibit lower mean flooding and smaller ranges of flooding values than small continents. This effect is evident among Paleozoic continents, for which both mean and maximum flooding values decrease with increasing landmass area (figs. 6, 7). Small Paleozoic continents ($< 10^7$ km²) average about 50 percent flooding with a maximum > 90 percent, whereas large continents ($> 5 \cdot 10^7$ km²) average about 20 percent flooding with a maximum near 30 percent.

Modern continents exhibit rather less flooding than Paleozoic landmasses of equivalent area (fig. 6). As the Early-Middle Paleozoic world was largely unglaciated (Frakes, Francis, and Syktus, 1992; Hallam, 1992), a more meaningful comparison would be with a modern ice-free world in which global sealevel elevations were about 50 m higher than at present (Harrison, 1990). However, the flooding values of Africa (6 percent), North America (22 percent), South America (17 percent), and Australia (29 percent) still fall below mean values for area-equivalent Paleozoic landmasses, and Eurasia alone (23 percent) approaches the mean value for a Paleozoic counterpart (fig. 6). Limited modern continental flooding may be due to: (1) a present-day eustatic elevation that is low with respect to its long-term mean owing to reduced mid-ocean ridge

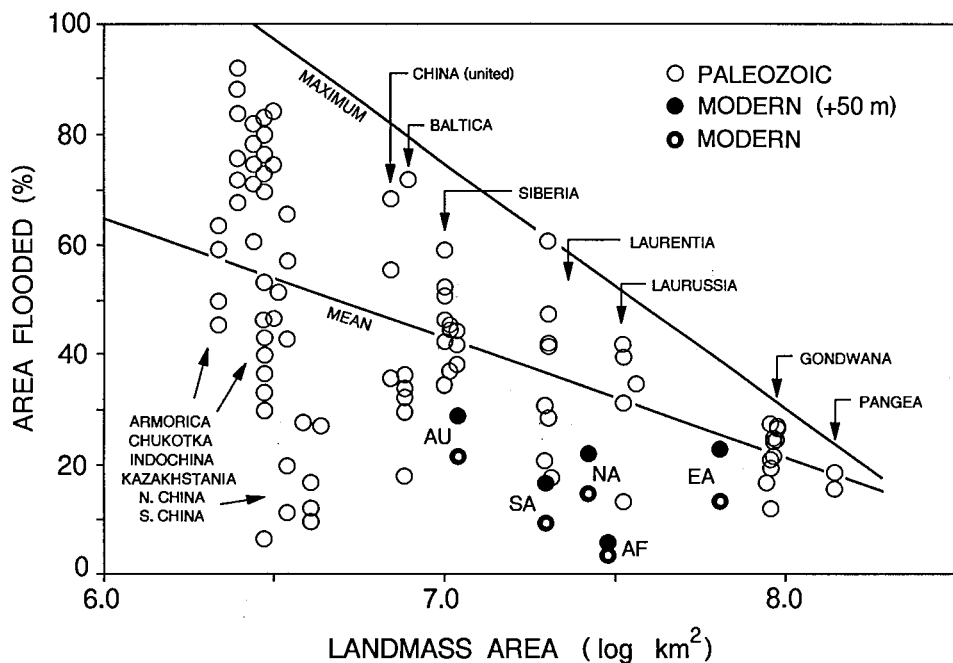


Fig. 6. Flooding versus landmass area for Paleozoic and modern continents. For Paleozoic continents, mean and maximum flooding decrease with increasing landmass area. For modern continents, flooding values are shown with respect to both present sealevel (circles with dots) and sealevel in an ice-free modern world (+50 m; solid circles). Modern continents: Australia (AU), South America (SA), North America (NA), Africa (AF), and Eurasia (EA). Note that modern continents generally exhibit lower degrees of flooding than Paleozoic landmasses of equivalent area.

spreading rates (Pitman, 1978), large areas of old oceanic lithosphere (Heller and Angevine, 1985), or some related factor, or (2) a general steepening of continental topography owing to decreased tectonic attenuation or increased stabilization of land surfaces by vegetation. Modern continents as a group do not show a strong correlation between landmass area and degree of flooding, and deviations from a straight-line relationship may reflect hypsometric disequilibrium of individual continents.

Landmass area is related not only to mean flooding but also to flooding range. Flooding range (that is, the standard deviation range of flooding values) is small for large Paleozoic continents, becoming generally larger, and more variable, for small Paleozoic continents (fig. 7). Large continents such as Pangea and Gondwana exhibit flooding variabilities of less than 5 percent, mid-sized continents such as Laurentia and Siberia 5 to 15 percent, and small continents such as Armorica and North China 5 to 25 percent. Low flooding variabilities for Chukotka and Indochina (<5 percent) result from temporally-invariant flooding esti-

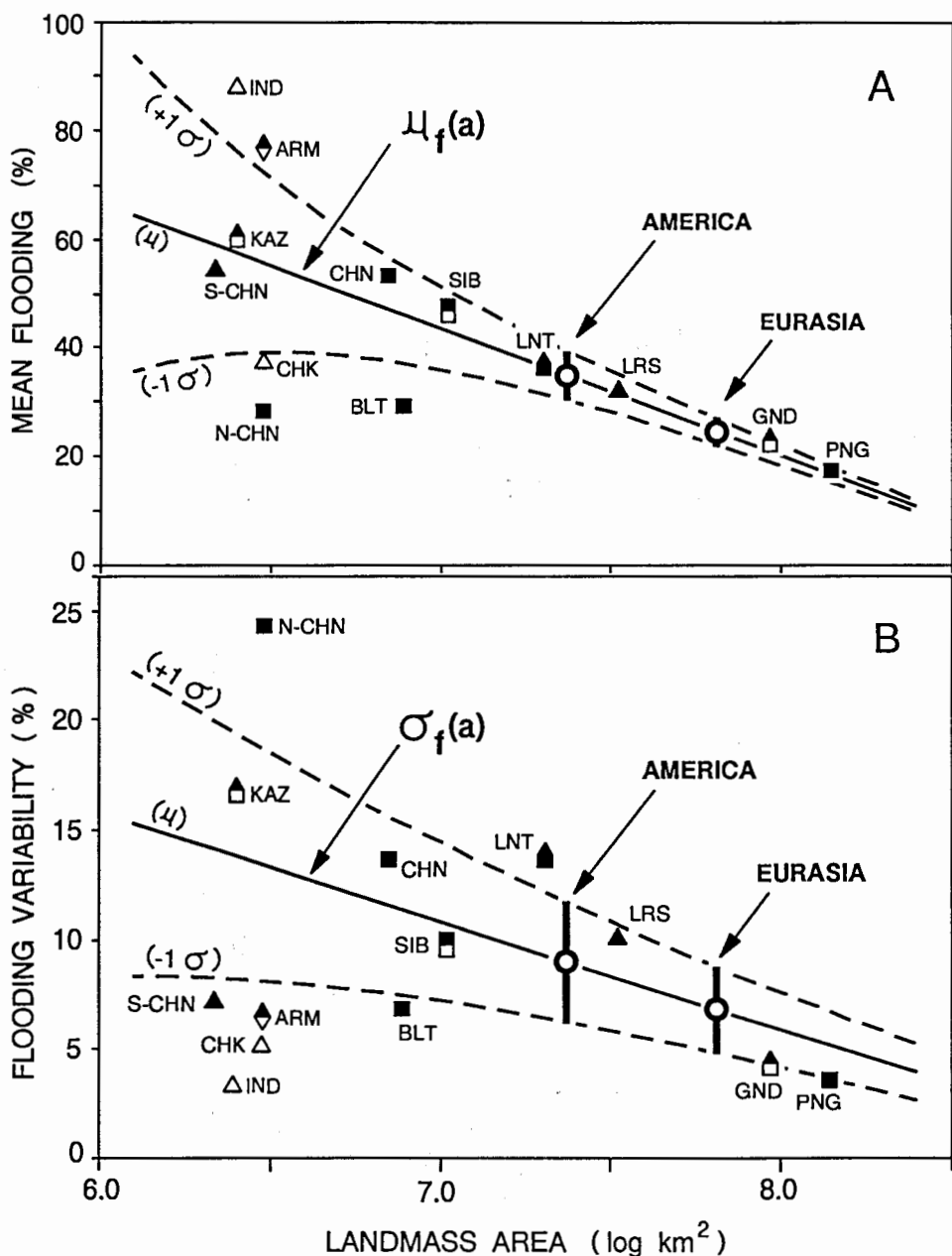


Fig. 7. Mean flooding and flooding ranges for Paleozoic continents. Both (A) mean flooding, $\mu_f(i)$, and (B) flooding range, $\sigma_f(i)$, decrease and exhibit less variability with increasing landmass area. These relationships are used to estimate "expected" means and ranges of flooding values for hypsometric analogs. Paleozoic continents equivalent in area to modern Eurasia and America would exhibit flooding ranges of 25 ± 7 and 35 ± 9 percent, respectively (open circles). Uncertainty limits for expected means and ranges of flooding values (solid vertical bars) are based on $\pm 1 \sigma$ regression lines (dashed).

mates owing to lack of detailed stratigraphic information rather than from genuinely small ranges of flooding values (fig. 7).

Scaling of paleocontinental hypsometries.—The procedure we use in dimensional scaling of paleocontinental hypsometries is based on relationships of landmass area to hypsometry and flooding. Because large landmasses exhibit less variability in hypsometric character and flooding range than small landmasses (figs. 6, 7), large modern continents in approximate “hypsometric equilibrium” may be good analogs for Paleozoic continents of comparable area. This application of uniformitarianism with respect to Phanerozoic continental geomorphology is probably the most important but least testable assumption underlying our methodology.

The basic scaling procedure using a modern continental analog involves determining two parameters for a Paleozoic landmass of equivalent area: (1) an “expected” mean flooding value, and (2) an “expected” range of flooding values. Once the mean and range of flooding for an area-equivalent Paleozoic landmass have been estimated, these values can be converted to absolute elevations using the hypsometry of the modern analog. The elevation range thus determined represents the estimated range of Paleozoic eustatic fluctuations based on that analog, to which the entire set of Paleozoic continental hypsometric chords is scaled (fig. 4B). Choice of a suitable hypsometric analog is important because it is the primary determinant of paleo-hypsometric and -eustatic elevations.

We estimated means and ranges of flooding values for two modern hypsometric analogs, Eurasia and America. Based on areas of 7.8 and 7.4 log km² for these two continents, area-equivalent Paleozoic landmasses would exhibit mean flooding values of 24.7 and 34.8 percent (fig. 7A), flooding variabilities of 6.7 and 8.8 percent (fig. 7B), and flooding ranges of 18.0 to 31.4 and 26.0 to 43.6 percent, respectively. Conversion of flooding values to elevations using the hypsometric curves of the modern analogs yields mean Paleozoic eustatic elevations of +60 m and +160 m and elevation ranges of 24 to 102 and 96 to 224 m for the Eurasian and American analogs, respectively (fig. 8). Although modern Eurasia and the Americas (North and South) have similar hypsometries (fig. 5), differences in their size and, hence, proximity to “expected” mean flooding values (fig. 6) are the source of large differences in resultant Paleozoic elevation estimates: the Eurasian analog is much closer than the American to the mean flooding value for an area-equivalent Paleozoic landmass (fig. 6) and, thus, yields a mean Paleozoic eustatic elevation (+60 m) only slightly above that of a modern ice-free world (+50 m). This makes clear the implications of choosing a Eurasian versus an American hypsometric model: the former implies that modern sealevel elevations are rather typical for the Phanerozoic, whereas the latter implies that they are anomalously low.

Analysis of Paleozoic Sea-Level Elevations

Calculation of sealevel elevations.—Following construction and scaling of coastal hypsometric chords for Paleozoic landmasses, calculation of

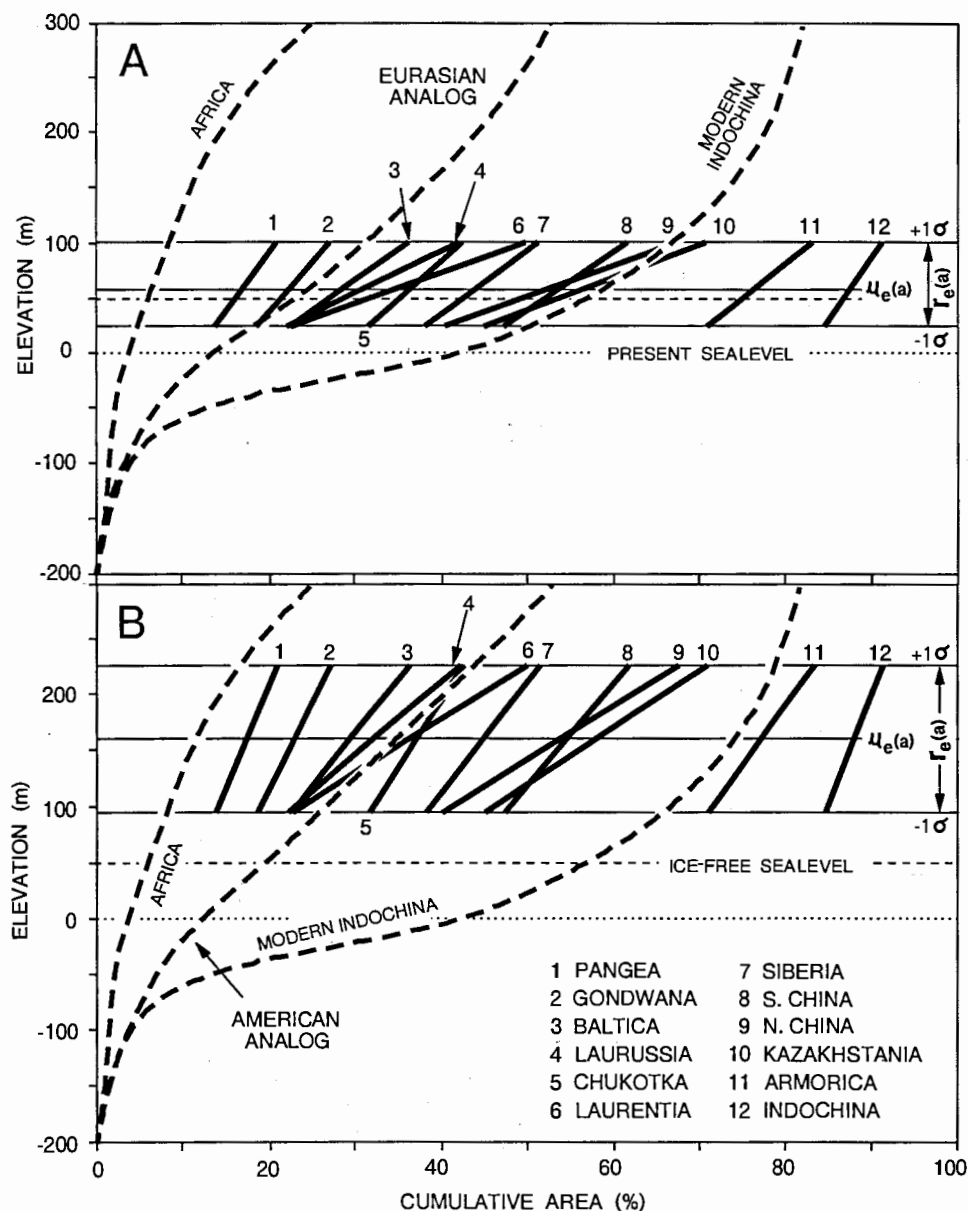


Fig. 8. Scaled hypsometric chords of Paleozoic continents using Eurasian (A) and American (B) analogs. The Eurasian model yields a mean elevation of +60 m and an elevation range of 24 to 102 m, whereas the American model yields a mean elevation of +160 m and an elevation range of 96 to 224 m. The area-elevation curves of modern Africa and Indochina bracket the coastal hypsometries of most Paleozoic continents. Note that use of an American analog results in steeper paleocontinental hypsometries and higher sealevel elevations than use of a Eurasian analog.

sealevel elevations for each continent by epoch is possible (fig. 1). This involves conversion of flooding values to sealevel elevations using the characteristic hypsometric chord of each paleocontinent:

$$S(ij) = m(i) \cdot F(ij) + b(i) \quad (7)$$

where $S(ij)$ is the sealevel elevation estimate for continent i at epoch j . For example, Laurentia has mean flooding values of 21, 32, and 48 percent for the Early, Middle, and Late Cambrian, respectively (table 1), yielding sealevel elevation estimates of 20, 45, and 90 m for the Eurasian analog or 80, 130, and 220 m for the American analog (fig. 9). Elevation estimates are not biased by use of linear hypsometric chords rather than continuously varying curves: although modern continental hypsometries are strongly non-linear over their complete elevation ranges, deviations from linearity are small within the elevation range of Phanerozoic eustasy (fig. 5), and significant non-linearity would develop only at extreme flooding values (for example, $> \mu_F(i) \pm 2\sigma$).

Once individual continental sealevel elevations have been estimated, Paleozoic eustatic elevations may be determined by one of several methods. In theory, each paleocontinent is an independent recorder of eustasy having equal validity. Therefore, global sealevel elevations may be calculated as a simple unweighted average of individual continental sealevel elevations by epoch:

$$S(wj) = i \sum_1^m S(ij)/m \quad (8)$$

where $S(wj)$ is the unweighted estimate of eustatic elevation, and m is the number of continents extant during epoch j . However, variance among paleocontinental sealevel estimates is related to flooding data quality: on average, elevation estimates based on excellent- or good-quality data deviate by 40 to 45 m from the global mean, whereas estimates based on poor-quality data deviate by 62 m (fig. 10). Therefore, we prefer eustatic estimates reflecting data quality:

$$S(wj) = i \sum_1^m [S(ij) \cdot Q(ij)] / i \sum_1^m Q(ij) \quad (9)$$

where $S(wj)$ is the quality-weighted estimate of eustatic elevation, and $Q(ij)$ is the weighting factor applied to the flooding estimate for continent i at epoch j . Weighting factors were assigned according to flooding data quality: excellent = 1.0, good = 0.5, fair = 0.33, and poor = 0.125 (arbitrary values).

Although sealevel estimates cluster to some degree for most epochs, differences remain between individual continental sealevel elevations

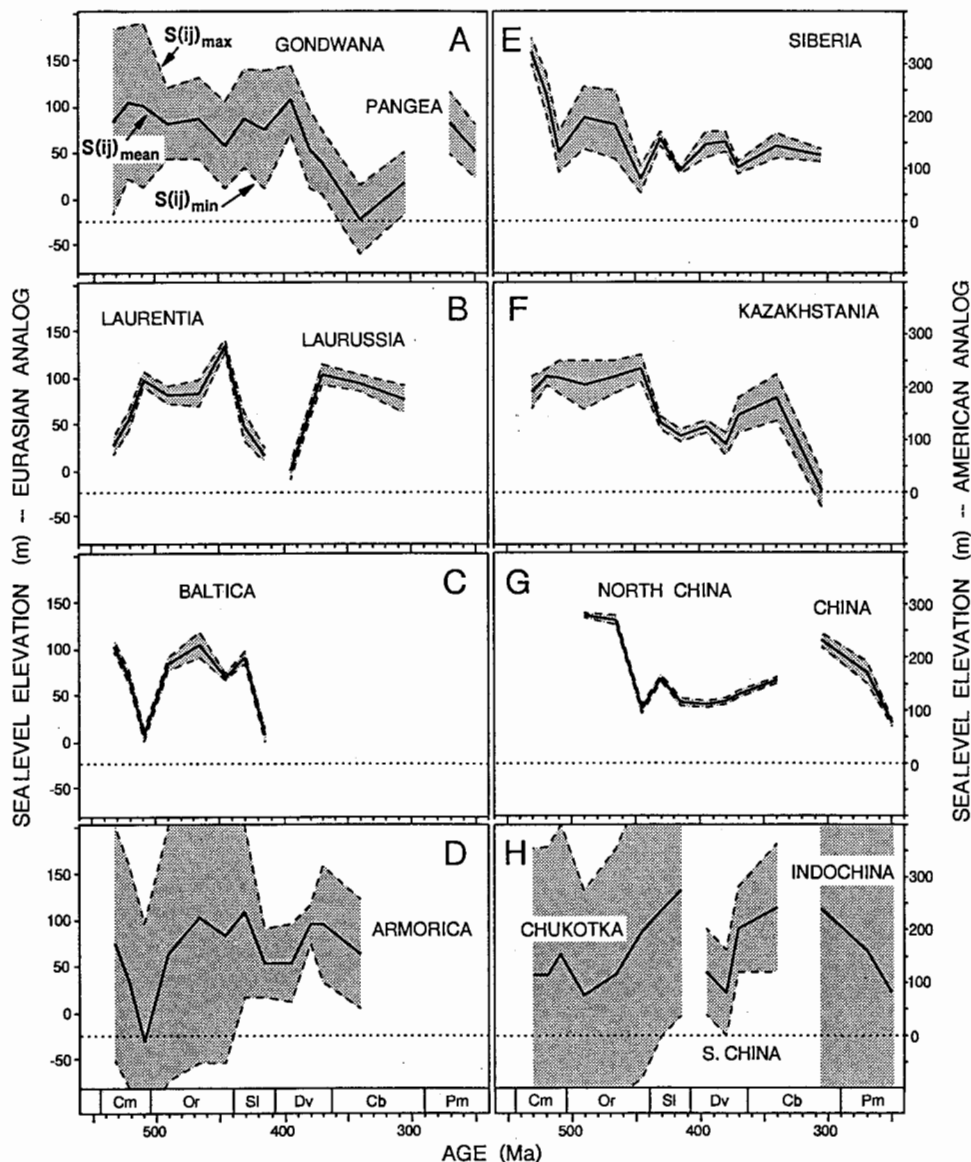


Fig. 9. Sealevel elevations for individual Paleozoic continents. Estimates are based on the "most-likely" or mean flooded area ($F(ij)_{\text{mean}}$; solid line) bracketed by minimum and maximum flooding values ($F(ij)_{\text{min}}$ and $F(ij)_{\text{max}}$; dashed lines). Secular sealevel trends are significant where elevation changes exceed the uncertainty range. Elevation scales are shown for both Eurasian (left) and American (right) analogs.

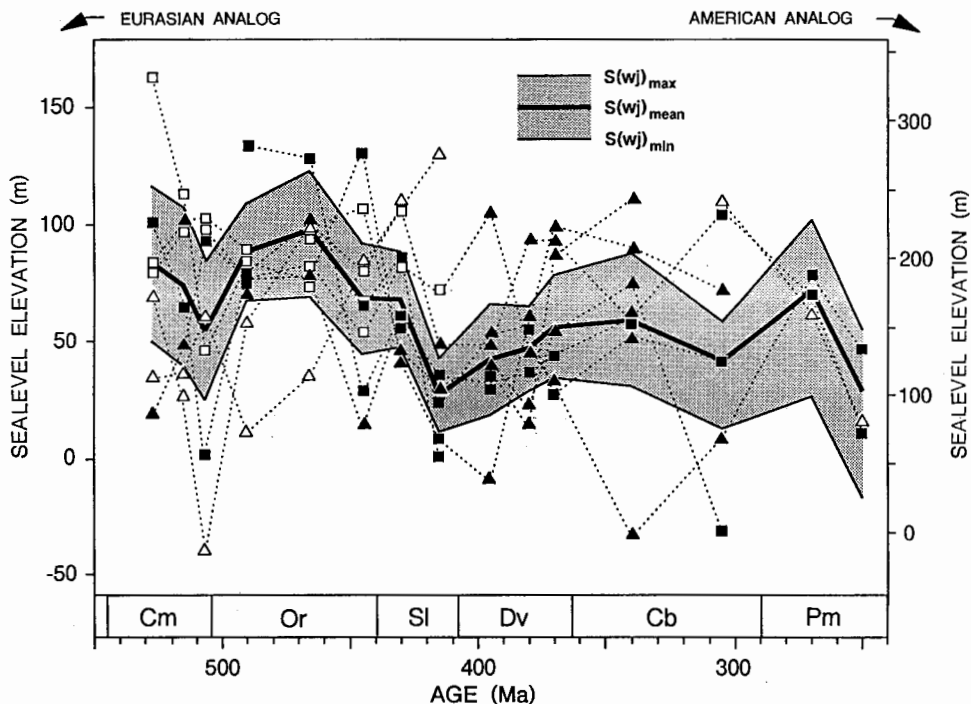


Fig. 10. Global and stacked continental sealevel elevations for the Paleozoic. Symbols on continental sealevel curves (dotted) represent data quality; refer to figure 3 for meaning of symbols and to figure 9 for identification of paleocontinents. The mean global curve (heavy solid line) is a quality-weighted average of continental sealevel elevations using weights of 1.0 for excellent (solid squares), 0.5 for good (solid triangles), 0.33 for fair (open squares), and 0.125 for poor flooding data (open triangles). The uncertainty range for global sealevel elevations (shaded) is based on minimum and maximum flooding values for all paleocontinents at each epoch (fig. 3). Elevation scales are shown for both Eurasian (left) and American (right) analogs.

and the global mean. These differences may be quantified as "elevation residuals":

$$\Theta S(ij) = S(ij) - S(wj) \quad (10)$$

where $\Theta S(ij)$ is the difference between the sealevel estimate for continent i and the global mean at epoch j . Generally, high (low) flooding values yield positive (negative) elevation residuals that may be interpreted as a reflection of broad epeirogenic crustal subsidence (uplift). The maximum amplitude of elevation residuals is about ± 90 m (± 150 m), slightly less than the range of eustatic fluctuations, that is, 100 ± 40 m (225 ± 75 m) for the Eurasian (American) analog. Elevation residuals for each Paleozoic landmass and discussion of their origin and significance are given in Algeo and Sestavinsky (1995).

Error analysis.—Calculated Paleozoic sealevel elevations are subject to four potential sources of error. These represent uncertainties in: (1) paleocontinental flooding estimates, (2) suitability of specific modern hypsometric analogs, (3) the expected mean flooding value of an area-equivalent Paleozoic landmass, and (4) the expected flooding range of that landmass. The magnitude of the first source is unique to each paleocontinent at each epoch, whereas those of the latter three are common to all paleocontinents at all epochs. To evaluate the significance of these error sources, we will estimate uncertainty ranges for each parameter and calculate their potential effects on sealevel elevations.

Uncertainty in flooding estimates is accounted for through use of minimum, mean, and maximum values (fig. 3). The width of the uncertainty ranges thus defined is a function of the quality and completeness of available stratigraphic data. Landmasses with good to excellent data (for example, Laurentia, Baltica, or North China) exhibit narrow uncertainty ranges, whereas those with poor to fair data (for example, Chukotka, Indochina, and Armorica) exhibit broad uncertainty ranges. The width of flooding uncertainty ranges (fig. 3) is mirrored generally by those for sealevel estimates (fig. 9). As a rule, resultant sealevel trends are valid if secular variation exceeds the calculated uncertainty range. For eustatic elevations, uncertainty ranges were calculated as a function of the minimum and maximum flooding values of paleocontinents, a procedure that compounds errors associated with individual continental flooding records and maximizes the width of resultant eustatic uncertainty ranges (fig. 10).

Parameters related to vertical scaling of paleocontinental hypsometric chords, that is, choice of a modern area-elevation analog and expected values for the mean and range of flooding of an area-equivalent Paleozoic landmass, represent "fixed" potential sources of error, because they are applied uniformly to all conversions of flooding values. It is difficult to evaluate uncertainties in the suitability of specific modern hypsometric analogs because so few are available. The Eurasian and American analogs have similar hypsometries (figs. 5, 8) but yield divergent sealevel estimates (fig. 9) owing to differences in landmass area (figs. 6, 7). Although unclear whether these two analogs exhibit the full range of potential hypsometric variation for large landmasses in "hypsometric equilibrium," considerations related to the steepness of Paleozoic global hypsometries suggest that the Eurasian and American analogs may represent reasonable lower and upper limits on such variation (see discussion below).

Uncertainties in expected values for the mean and range of flooding of an area-equivalent Paleozoic landmass may be estimated from landmass area-flooding relationships (fig. 7). Both parameters exhibit strong negative co-variance with landmass area at areas greater than 10^7 km², permitting calculation of uncertainty limits for paleocontinents of a specified size. Uncertainty ranges for expected mean flooding values are 34.8 ± 4.5 and 24.7 ± 2.4 percent (fig. 7A), and those for expected

flooding ranges are 8.8 ± 2.7 and 6.7 ± 2.0 percent based on the American and Eurasian analogs, respectively (fig. 7B). Because these three "fixed" sources of uncertainty are global in their operation, their potential effect on sealevel elevation estimates are illustrated only for Laurentia/Laurussia (fig. 11). The most important source is the choice of hypsometric analog, because the Eurasian and American analogs yield sealevel elevations that differ systematically by about 100 m. Uncertainties in the expected mean and range of flooding values for an area-equivalent Paleozoic landmass result in comparatively modest uncertainty ranges, that is, about ± 20 and ± 35 m for the Eurasian and American analogs, respectively (fig. 11).

Comparison with Vail and Hallam eustatic curves.—Our Paleozoic eustatic curve (fig. 12) is similar in general form to the Paleozoic portions of the Vail, Mitchum, and Thompson (1977) and Hallam (1984) curves. All three exhibit Caledonian and Appalachian-Hercynian eustatic cycles, terminated by major regressions in the Late Silurian and Late Permian,

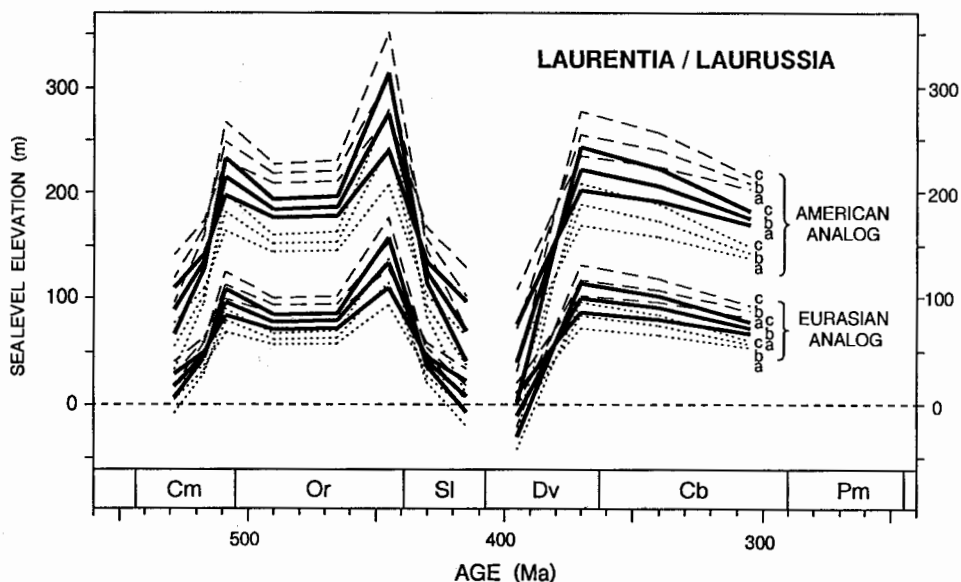


Fig. 11. Error analysis for "fixed" sources of potential error in Paleozoic sealevel calculations, that is, choice of a modern hypsometric analog and expected values for the mean and range of flooding for an area-equivalent Paleozoic landmass. Any error in these sources affects all sealevel calculations equally, because they are applied uniformly to all conversions of flooding values. Shown are 18 secular sealevel trends for Laurentia/Laurussia based on the American and Eurasian analogs and all possible permutations of minimum (dotted), mean (solid), and maximum (dashed) values of expected mean flooding (fig. 7A) and minimum (a), mean (b), and maximum (c) values of expected flooding range (fig. 7B). Other paleocontinents exhibit similar uncertainty ranges for sealevel elevations (not shown). Although potentially inducing shifts in Paleozoic sealevel elevations of up to ± 100 m, none of these three sources of uncertainty affects secular sealevel trends.

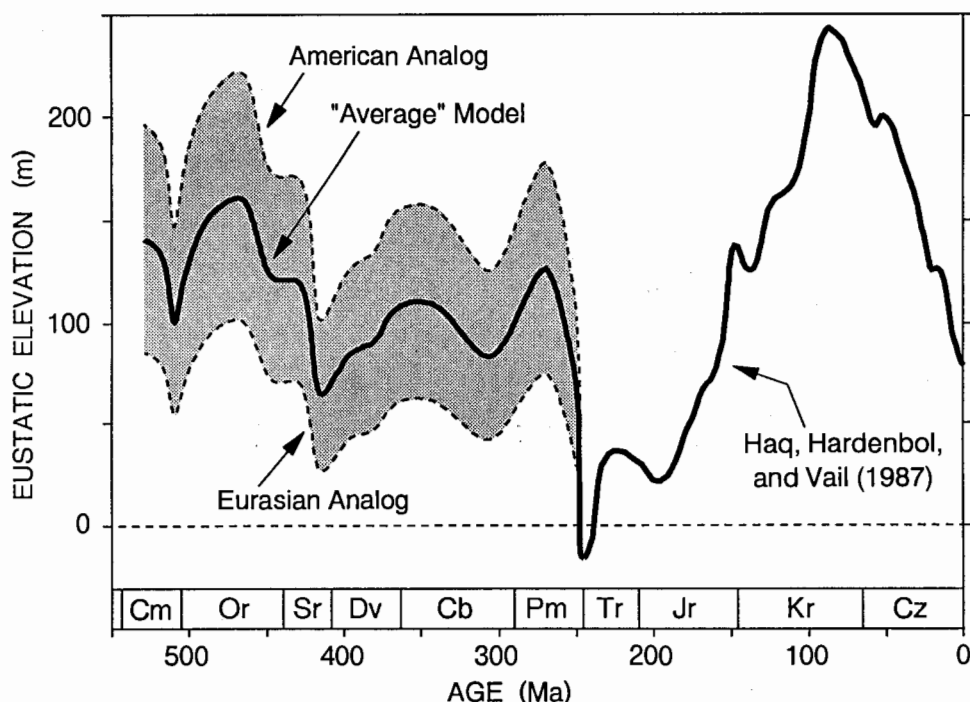


Fig. 12. Proposed Phanerozoic eustatic curve. The Paleozoic portion is based on this study, and the Mesozoic-Cenozoic portion is from Haq, Hardenbol, and Vail (1987; their long-term curve smoothed by 80 passes of a 0.25:0.5:0.25 filter). The Paleozoic curve (solid line) represents an "average model" that uses mean values of continental flooding ($F(ij)_{\text{mean}}$), expected mean flooding ($\mu_r(a)$), expected flooding range ($r_r(a)$), and a hypsometric model that is intermediate between the Eurasian and American analogs; upper and lower uncertainty limits (dashed lines) are based upon the American and Eurasian analogs, respectively.

respectively. The most salient difference between the curves pertains to Cambrian sealevel trends. The Vail and Hallam curves illustrate a strong Cambrian transgression, based largely on stratigraphic data from Laurentia (compare Cook and Bally, 1975). However, slow transgression of Laurentia during the Middle-Late Cambrian may have been due to the presence of subsiding passive margins on both continental flanks (Bond, Nickerson, and Kominz, 1984), the consequence of its central position in a disintegrating Late Proterozoic supercontinent (Dalziel, 1991). This raises the possibility that Laurentia had a flooding history unrepresentative of global Paleozoic trends, a hypothesis supported by anomalously large elevation residuals (Algeo and Sessler, 1995) and by absence of a significant eustatic component to total sealevel variance (table 4). In contrast to the Vail and Hallam curves, our Paleozoic eustatic trend illustrates a weak Cambrian regression, which is consistent with wide-

spread deposition of Lower-Middle Cambrian marine sediments on the Siberian, East European, Arabian, and Chinese platforms (Ronov, Khain, and Sestavinsky, 1984; McKerrow, Scotese, and Brasier, 1992).

Although exhibiting similar trends, major differences exist among the three Paleozoic eustatic curves with regard to absolute sealevel elevations (fig. 12). Estimates for the mid-Ordovician highstand are +600 m in the Hallam curve, +300 m in the Vail curve, and +100 to +225 m in this study. In comparison, the Late Cretaceous highstand has been estimated at +175 to +270 m using a variety of methods (Bond, 1979; Harrison and others, 1983; Kominz, 1984; Haq, Hardenbol, and Vail, 1987; Sahagian, 1987, 1988; Engebretson and others, 1992). Differences in elevation estimates for the Paleozoic and Mesozoic-Cenozoic eustatic highstands have different geotectonic implications. Assuming dominant control of first-order eustatic cycles by mid-ocean-ridge volume (Donovan and Jones, 1979; Harrison, 1990), the Vail and Hallam curves imply substantially faster spreading rates and/or lengthier ridges during the Paleozoic than during the Mesozoic-Cenozoic (compare Larson, 1991). Our results imply that mid-ocean ridge volumes have exhibited the same range of variation throughout the Phanerozoic, which is consistent with the observation that continental freeboard has been relatively constant since at least the Late Archean (Wise, 1974; Schubert and Reymer, 1985; Galer, 1991; Kasting and Holm, 1992).

Revision of Paleozoic eustatic estimates also has important implications for geochemical and paleoclimatic models in which eustasy has been used as a proxy for other parameters, for example, mid-ocean ridge spreading rates, submarine hydrothermal fluxes, and area-dependent continental weathering rates (Gaffin, 1987; Berner, 1991, 1994; Berner and Rye, 1992; Railsback, 1992). In order to assist global modelling efforts, we present a first-order Phanerozoic eustatic curve, combining results of this study for the Paleozoic with a smoothed version of the long-term eustatic curve of Haq, Hardenbol, and Vail (1987) for the Mesozoic-Cenozoic (fig. 12). The Paleozoic portion of the curve is based on mean values for all parameters, including a hypsometric model that averages the Eurasian and American analogs. The most compelling reason for adopting an intermediate area-elevation model is that the two modern analogs yield approximate lower and upper limits on the range of acceptable global hypsometries (see discussion below).

ANALYSIS OF VARIANCE IN FLOODING AND SEALEVEL DATA

Variance among the flooding records of individual paleocontinents includes hypsometric, eustatic, and residual components. In contrast, variance among paleocontinental sealevel records includes only eustatic and residual components because hypsometric factors were removed in the process of converting flooding values to sealevel elevations. For both records, the hypsometric component of variance is unique to each landmass (that is, spatially variant, temporally invariant), the eustatic

component is common to all landmasses (that is, temporally variant, spatially invariant), and the residual component is unique to each landmass at each epoch (that is, both temporally and spatially variant). The source of the residual component includes both secular changes in paleocontinental hypsometry and errors in flooding estimates. These relationships can be expressed as:

$$Vf_t(w) = Vf_e(w) + Vf_h(w) + Vf_r(w) \quad (11)$$

$$Vs_t(w) = Vs_e(w) + Vs_r(w) \quad (12)$$

where $Vf_t(w)$ and $Vs_t(w)$ are total variances, $Vf_e(w)$ and $Vs_e(w)$ are variances associated with eustatic factors, and $Vf_r(w)$ and $Vs_r(w)$ are variances associated with residual factors in flooding and sealevel elevation records, respectively, and $Vf_h(w)$ is variance associated with hypsometric factors in flooding records.

The procedure utilized above to reconstruct hypsometric chords for individual Paleozoic continents assigns as much of the total variance in flooding records as possible to differences in time-averaged mean coastal hypsometry, thereby maximizing the fractional contribution of eustatic variance to total variance in the resultant continental sealevel records. However, calculation of the reduction in total variance resulting from conversion of flooding values to sealevel elevations (that is, removal of the hypsometric component) is not straight-forward owing to non-equivalence of the scales of measurement of flooding and sealevel elevation data. We make a two-step calculation, first determining the fraction of total variance in the Paleozoic flooding and sealevel records attributable to eustatic factors and then setting these fractions equal to determine the ratio of total variances in the flooding and sealevel datasets. For the Paleozoic as a whole, the eustatic fractions of total variance may be calculated as:

$$'Vf_e(w) = j \sum_1^n [F(w_j) - \mu_F(w)]^2 \bigg/ i \sum_1^m j \sum_1^n [F(ij) - \mu_F(w)]^2 \cdot m \quad (13)$$

$$'Vs_e(w) = j \sum_1^n [S(w_j) - \mu_S(w)]^2 \bigg/ i \sum_1^m j \sum_1^n [S(ij) - \mu_S(w)]^2 \cdot m \quad (14)$$

where $'Vf_e(w)$ and $'Vs_e(w)$ are the fractional contributions of eustatic factors to total variance in the flooding and sealevel datasets, respectively, and $\mu_F(w)$ and $\mu_S(w)$ are mean Paleozoic flooding and sealevel elevation for the world. The fractional contributions of eustasy to total variance are 0.009 and 0.18 for the flooding and sealevel datasets, respectively. Because the amount of variance associated with the eustatic component must be the same for both sets of data, these fractional values may be set

equal to determine the ratio of total flooding variance to total sealevel variance:

$$Vf_t(w)/Vs_t(w) = 'Vs_e(w)/'Vf_e(w) \quad (15)$$

which yields a ratio of about 20:1. The amount of variance associated with the residual component also must be the same for both datasets, and assigning arbitrary values of 1.0 to $Vs_t(w)$ and 0.18 to both $Vs_e(w)$ and $Vf_e(w)$ permits calculation of the remaining variances as:

$$Vf_r(w) = Vs_r(w) = Vs_t(w) - Vs_e(w) \quad (16)$$

$$Vf_h(w) = Vf_t(w) - Vf_e(w) - Vf_r(w) \quad (17)$$

yielding values of 0.82 for $Vf_r(w)$ and $Vs_r(w)$ and 19.0 for $Vf_h(w)$. Thus, total variance has been reduced by 95 percent (20.0-1.0) in the process of converting flooding values to sealevel elevations using time-averaged mean coastal hypsometries, and, of the remaining 5 percent of flooding variance (representing 100 percent of sealevel variance), about one fifth (0.18) is associated with eustatic factors and four fifth (0.82) with residual factors.

In the second part of our analysis of variance, we examine the relative contributions of eustatic and residual factors to total variance in the sealevel elevation records of individual Paleozoic continents:

$$'Vs_r(i) = j \sum_1^n [S(ij) - S(w)]^2 \bigg/ j \sum_1^n [S(ij) - \mu_s(w)]^2 \quad (18)$$

$$'Vs_e(i) = 1 - Vs_r(i) \quad (19)$$

where $'Vs_r(i)$ and $'Vs_e(i)$ are the fractional contributions of residual and eustatic factors, respectively, to variance in sealevel elevations of continent i . Values of $'Vs_r(i)$ and $'Vs_e(i)$ were calculated using both unweighted and quality-weighted global sealevel elevations (table 4). Many continents having good to excellent flooding records exhibit relatively large eustatic components of variance, for example, Baltica (54-61 percent), North China/United China (40-47 percent), Kazakhstania (30-45 percent), and Siberia (25-35 percent). On the other hand, Gondwana/Pangea and Laurentia/Laurussia contain almost no eustatic component (0 and 3-7 percent, respectively). For paleocontinents having residual components greater than 1.0, the mean eustatic trend (fig. 10) does not account for any of the variance in that continent's sealevel record and, in fact, has contributed additional variance to it. The large residual components of sealevel variance for Chukotka and Indochina are probably due to unreliable flooding data (fig. 3).

Several important points emerge from this analysis. First, for continents having high-quality flooding records, between one third and

TABLE 4
Sources of variance in continental sealevel records*

Continent	Unweighted SL [#]		Weighted SL [#]	
	Eustatic	Residual	Eustatic	Residual
Gondwana/Pangea	-0.01	1.01	-0.01	1.01
Laurentia/Laurussia	0.07	0.93	0.03	0.97
Baltica	0.54	0.46	0.61	0.39
Siberia	0.25	0.75	0.35	0.65
Armorica	0.17	0.83	0.00	1.00
Chukotka	-0.59	1.59	-1.23	2.23
Kazakhstan	0.30	0.70	0.45	0.55
N. China/United China	0.40	0.60	0.47	0.53
S. China	0.26	0.74	0.21	0.79
Indochina	0.20	0.80	-0.11	1.11

* Fractional contributions of eustatic and residual components to total variance in continental sealevel elevations, $V_{se}(i)$ and $V_{sr}(i)$, respectively; negative values reflect increased deviation from global mean.

Calculations based on unweighted and quality-weighted global mean sealevel elevations, $S(wj)$ and $S(wj)$, respectively.

two-thirds of sealevel variance resides in eustatic factors and a comparable amount in residual factors. Second, for continents having low-quality flooding records, residual variances in excess of 1.0 suggest that data quality is the limiting factor and that calculated secular sealevel trends may be erroneous. Third, the sealevel record of Laurentia/Laurussia, although widely used as a global standard for Paleozoic sealevel trends (Wise, 1974; Vail, Mitchum, and Thompson, 1977; Gurnis, 1990), contains a negligible eustatic component and is controlled primarily by residual factors of probable epeirogenic origin (Algeo and Seslavinsky, 1995). These considerations demonstrate the importance of using multiple independent data sources in paleo-eustatic analysis.

MODERN AND ANCIENT GLOBAL HYPSONOMETRIES

The American and Eurasian analogs yield substantially different ranges of eustatic elevations and, therefore, cannot both be correct. One method of evaluating the relative validity of the two models is by considering their effect on global hypsometry. Global hypsometry is the areally-weighted mean of the area-elevation distributions of all extant land-masses at a given time (Harrison and others, 1983). Given information regarding individual continental hypsometries over some range of elevations, it is possible to reconstruct global hypsometry for the same elevation range. The procedure is to calculate: (1) a global flooding range for a given epoch, and (2) a global hypsometric chord using the same elevation

range as for individual continental hypsometric chords. Global flooding ranges may be calculated as:

$$\mu_F(wj) = i \sum_1^m [\mu_F(i) \cdot A(ij)] / i \sum_1^m A(ij) \quad (20)$$

$$\sigma_F(wj) = i \sum_1^m [[\mu_F(i) \pm \sigma_F(i)] \cdot A(ij)] / i \sum_1^m A(ij) \quad (21)$$

$$r_F(wj) = \mu_F(wj) \pm \sigma_F(wj) \quad (22)$$

where $\mu_F(wj)$, $\sigma_F(wj)$, and $r_F(wj)$ are the mean, standard deviation, and range, respectively, of global flooding values at epoch j . Global hypsometric chords are calculated as:

$$m(wj) = r_S(w)/r_F(wj) \quad (23)$$

$$b(wj) = \mu_S(w) - m(wj) \cdot \mu_F(wj) \quad (24)$$

where $m(wj)$ and $b(wj)$ are the slope and y-intercept, respectively, of the global hypsometric chord at epoch j .

Reconstruction of global hypsometric chords for each Paleozoic epoch yields important insights regarding the secular evolution of global hypsometry and the significance of selecting an American versus a Eurasian analog. First, global hypsometric chords for the 13 epochs from the Early Cambrian to the Late Carboniferous are virtually indistinguishable (irrespective of choice of analog), whereas Early and Late Permian global hypsometries are steeper than those of earlier epochs (fig. 13). This implies an abrupt steepening of global hypsometry associated with formation of Pangea (Harrison and others, 1981; Hay and others, 1981). Reduced global flooding during the Permian probably resulted from both steeper global hypsometry (fig. 13) and an increase in ocean-basin volume owing to orogenic thickening of continental lithosphere (Wyatt, 1984; Algeo and Wilkinson, 1991).

Second, choice of an American versus a Eurasian analog has very different implications for the hypsometric character of the Paleozoic world. The elevation range associated with an American analog (that is, 96-224 m) suggests that coastal hypsometries for the Cambro-Carboniferous were similar to that of the modern world and those of the Permian world were steeper than at present (fig. 13). In contrast, the elevation range associated with a Eurasian analog (that is, 24-102 m) implies that coastal hypsometries of the Cambro-Carboniferous were gentler than at present, and those of the Permian were similar to that of the modern world. In our opinion, the American and Eurasian analogs represent approximate upper and lower limits on the range of probable global hypsometries for the Paleozoic. The dispersed condition of continents during much of the Early and Middle Paleozoic (Scotese and McKerrow, 1990) favors a global hypsometry no steeper than that produced by the American model, and continental amalgamation in a Permian supercon-

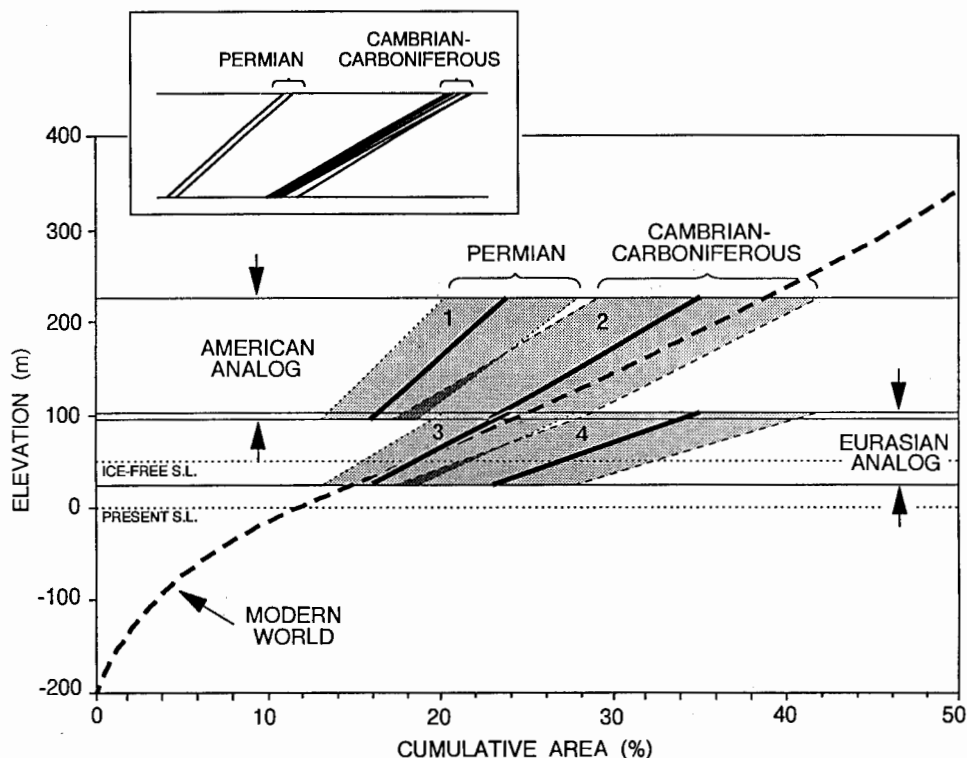


Fig. 13. Global hypsometric chords by epoch for the Eurasian and American analogs. Global hypsometries for the 13 epochs between the Early Cambrian and Late Carboniferous are similar (inset) and are represented by a single hypsometric chord in main part of figure. Global hypsometries of the Early-Late Permian are markedly steeper than those of the pre-Permian. Choice of modern hypsometric analog controls the elevation range and, hence, the overall steepness of Paleozoic hypsometric chords. Note that the area-elevation distribution of the modern world is similar to global hypsometries of the Cambro-Carboniferous using an American analog and to those of the Permian using a Eurasian analog.

continent favors a global hypsometry no gentler than that produced by the Eurasian model (Harrison and others, 1981). Thus, actual Paleozoic global hypsometries may have been intermediate between these limits, yielding a mean sealevel elevation of about +110 m and a range of about 60 to 160 m, which is our preferred model (fig. 12).

CONCLUSIONS

1. Comparative analysis of multiple Paleozoic continental flooding records permits partial reconstruction of paleocontinental and global hypsometries, calculation of individual continental and global sealevel elevations, and isolation of elevation residuals that may represent secular epirogenic motions.

2. Variance in Paleozoic continental flooding records includes contributions from long-term mean hypsometric (95 percent), eustatic (1 percent), and residual sources (4 percent; representing a combination of secular changes in hypsometry and errors in flooding estimates).

3. After removal of the hypsometric component of variance through conversion of flooding values to sealevel elevations, the eustatic component typically represents one third to two thirds of remaining variance for paleocontinents with high-quality flooding records and little or none of the remaining variance for those with low-quality flooding records.

4. The flooding record of Laurentia/Laurussia, although high-quality, exhibits almost no eustatic component to variance, making its use as a global standard for the Paleozoic questionable.

5. Scaling of paleocontinental hypsometric chords using Eurasian and American analogs results in mean Paleozoic sealevel elevations of +60 and +160 m and sealevel elevation ranges of 24 to 102 and 96 to 224 m, respectively. Thus, the elevation range of Paleozoic eustasy was probably comparable to that of the Mesozoic-Cenozoic, and previous estimates of Paleozoic highstands ranging from +300 to +600 m are probably incorrect.

6. Error analysis indicates that, owing to uncertainties in the suitability of specific modern hypsometric analogs and in the expected mean and range of flooding values for area-equivalent Paleozoic landmasses, the absolute elevation range of Paleozoic eustasy is in doubt by about ± 100 m.

7. Secular sealevel trends are well-defined for most paleocontinents and for the world as a whole, and their validity is not dependent on uncertainties in "fixed" parameters controlling vertical scaling of paleocontinental hypsometric chords.

8. Paleozoic continents exhibit strong inverse relationships between landmass area and both mean and maximum flooding values, underscoring the need for consideration of landmass area effects in paleo-eustatic analysis.

9. An abrupt steepening of global hypsometries occurred between the Late Carboniferous and Early Permian owing to continental suturing and formation of Pangea during the Appalachian-Hercynian Orogeny.

10. Eurasian and American analogs have profoundly different implications for global hypsometry: the former yields Cambro-Carboniferous hypsometries gentler than at present and Permian hypsometries similar to the modern world, whereas the latter yields Cambro-Carboniferous hypsometries similar to the present and Permian hypsometries steeper than in the modern world.

ACKNOWLEDGMENTS

We thank Bruce Wilkinson for support and assistance during the early phases of this project, George Klein, Leigh Royden, and Dork Sahagian for thoughtful reviews, and Lisa Trump for drafting services. Research funding was provided by a University of Cincinnati Research

Council grant to TJA and a Project Development Grant from the National Academy of Sciences to TJA/KBS.

REFERENCES

- Algeo, T. J., and Soslavinsky, K. B., 1995, Reconstructing eustatic and epeirogenic trends from Paleozoic continental flooding data, in Haq, B. U., editor, *Sequence Stratigraphy and Depositional Response to Eustatic, Tectonic and Climatic Forcing*: Dordrecht, Kluwer, in press.
- Algeo, T. J., and Wilkinson, B. H., 1991, Modern and ancient continental hypsometries: *Journal of the Geological Society of London*, v. 148, p. 643–654.
- Berner, R. A., 1991, A model for atmospheric CO₂ over Phanerozoic time: *American Journal of Science*, v. 291, p. 339–376.
- , 1994, Geocarb II: a revised model of atmospheric CO₂ over Phanerozoic time: *American Journal of Science*, v. 294, p. 56–91.
- Berner, R. A., and Rye, D. M., 1992, Calculation of the Phanerozoic strontium isotope record of the oceans from a carbon cycle model: *American Journal of Science*, v. 292, p. 136–148.
- Bond, G. C., 1976, Evidence for continental subsidence in North America during the Late Cretaceous global submergence: *Geology*, v. 4, p. 557–560.
- , 1978a, Speculations on real sea-level changes and vertical motions of continents at selected times in the Cretaceous and Tertiary Periods: *Geology*, v. 6, p. 247–250.
- , 1978b, Evidence for Late Tertiary uplift of Africa relative to North America, South America, Australia and Europe: *Journal of Geology*, v. 86, p. 47–65.
- , 1979, Evidence for some uplifts of large magnitude in continental platforms: *Tectonophysics*, v. 61, p. 285–305.
- Bond, G. C., and Kominz, M. A., 1991, Disentangling Middle Paleozoic sea level and tectonic events in cratonic margins and cratonic basins of North America: *Journal of Geophysical Research*, v. 96, p. 6619–6639.
- Bond, G. C., Nickerson, P. A., and Kominz, M. A., 1984, Breakup of a supercontinent between 625 Ma and 555 Ma: new evidence and implications for continental histories: *Earth and Planetary Science Letters*, v. 70, p. 325–345.
- Bowring, S. A., Grotzinger, J. P., Isachsen, C. E., Knoll, A. N., Pelechaty, S. M., and Kolosov, P., 1993, Calibrating rates of Early Cambrian evolution: *Science*, v. 261, p. 1293–1298.
- Burke, K., and Whiteman, A. J., 1973, Uplift, rifting and the breakup of Africa, in Tarling, D. J., and Runcorn, S. K., editors, *Implications of Continental Drift to the Earth Sciences*, v. 2: London, Academic Press, p. 735–755.
- Cogley, J. G., 1984, Continental margins and the extent and number of the continents: *Review of Geophysics and Space Physics*, v. 22, p. 101–122.
- , 1985, Hypsometry of the continents: *Zeitschrift für Geomorphologie, Supplementband*, v. 53.
- Cook, T. D., and Bally, A. W., editors, 1975, *Stratigraphic Atlas of North and Central America*: Princeton, New Jersey Princeton University Press, 272 p.
- Dalziel, I. W. D., 1991, Pacific margins of Laurentia and East Antarctica-Australia as a conjugate rift pair: evidence and implications for an Eocambrian supercontinent: *Geology*, v. 19, p. 598–601.
- Davies, T. A., and Worsley, T. R., 1981, Paleoenvironmental implications of oceanic carbonate sedimentation rates, in Warme, J. E., Douglas, R. G., and Winterer, E. L., editors, *The Deep Sea Drilling Project: A Decade of Progress*: Tulsa, Oklahoma, Society of Economic Paleontologists and Mineralogists, Special Publication 32, p. 169–179.
- Dennison, J. M., and Head, J. W., 1975, Sealevel variations interpreted from the Appalachian Basin Silurian and Devonian: *American Journal of Science*, v. 275, p. 1089–1120.
- Donovan, D. T., and Jones, E. J. W., 1979, Causes of world-wide changes in sea level: *Journal of the Geological Society of London*, v. 136, p. 187–192.
- Engelbreton, D. C., Kelley, K. P., Cashman, H. J., and Richard, M. A., 1992, 180 million years of subduction: *GSA Today*, v. 2, p. 93–100 (not incl.).
- Fischer, A. G., 1984, The two Phanerozoic supercycles, in Berggren, W. A., and Van Couvering, J. A., editors, *Catastrophes and Earth History*: Princeton, New Jersey, Princeton University Press, p. 129–150.
- Frakes, L. A., Francis, J. E., and Syktus, J. I., 1992, *Climate Modes of the Phanerozoic*: Cambridge, United Kingdom, Cambridge University Press, 274 p.
- Gaffin, S., 1987, Ridge volume dependence on seafloor generation rate and inversion using long term sealevel change: *American Journal of Science*, v. 287, p. 596–611.
- Galer, S. J. G., 1991, Interrelationships between continental freeboard, tectonics and mantle temperature: *Earth and Planetary Science Letters*, v. 105, p. 214–228.

- Gregor, B., 1985, The mass-age distribution of Phanerozoic sediments, in Snelling, N. J., editor, *The Chronology of the Geological Record*, Geological Society of London Memoir 10: Oxford, United Kingdom, Blackwell, p. 284–289.
- Gurnis, M., 1990, Bounds on global dynamic topography from Phanerozoic flooding of continental platforms: *Nature*, v. 344, p. 754–756.
- Hallam, A., 1977, Secular changes in marine inundation of USSR and North America through the Phanerozoic: *Nature*, v. 269, p. 769–772.
- , 1984, Pre-Quaternary sea-level changes: *Annual Review of Earth and Planetary Sciences*, v. 12, p. 205–243.
- , 1992, *Phanerozoic Sea-Level Changes*: New York, Columbia University Press, 266 p.
- Haq, B. U., Hardenbol, J., and Vail, P. R., 1987, Chronology of fluctuating sea levels since the Triassic: *Science*, v. 235, p. 1156–1167.
- Harland, W. B., Armstrong, R. L., Cox, A. V., Craig, L. E., Smith, A. G., and Smith, D. G., 1990, *A Geologic Time Scale 1989*: Cambridge, United Kingdom, Cambridge University Press, 263 p.
- Harrison, C. G. A., 1990, Long-term eustasy and epeirogeny in continents, in Revelle, R. R., and others, *Sea-Level Change*: Washington, D.C., National Academy Press, National Research Council, Studies in Geophysics, p. 141–158.
- Harrison, C. G. A., Brass, G. W., Saltzman, E., Sloan, J., II, Southam, J., and Whitman, J. M., 1981, Sea level variations, global sedimentation rates and the hypsographic curve: *Earth and Planetary Science Letters*, v. 54, p. 1–16.
- Harrison, C. G. A., Miskell, K. J., Brass, G. W., Saltzman, E. S., and Sloan, J. L., II, 1983, Continental hypsography: *Tectonics*, v. 2, p. 357–377.
- Hay, W. W., Barron, E. J., Sloan, J. L., II, and Southam, J. R., 1981, Continental drift and the global pattern of sedimentation: *Geologische Rundschau*, v. 70, p. 302–315.
- Heckel, P. H., 1986, Sea-level curve for Pennsylvanian eustatic marine transgressive-regressive depositional cycles along midcontinent outcrop belt, North America: *Geology*, v. 14, p. 330–334.
- Heller, P. L., and Angevine, C. L., 1985, Sea-level cycles during the growth of Atlantic-type oceans: *Earth and Planetary Science Letters*, v. 75, p. 417–426.
- Hutchison, C. S., 1989, The Palaeo-Tethyan realm and Indosinian orogenic system of Southeast Asia, in Sengör, A. M. C., editor, *Tectonic Evolution of the Tethyan Region*: Dordrecht, Kluwer, p. 585–643.
- Johnson, J. G., Klapper, G., and Sandberg, C. A., 1985, Devonian eustatic fluctuations in Euramerica: *Geological Society of America Bulletin*, v. 96, p. 567–587.
- Johnson, M. E., Kaljo, D., and Rong, J.-Y., 1991, Silurian eustasy, in Bassett, M. G., Lane, P. D., and Edwards, D., editors, *The Murchison Symposium (Proceedings of an international conference on the Silurian System): Special Papers in Palaeontology*, v. 44, p. 145–163.
- Kasting, J. F., and Holm, N. G., 1992, What determines the volume of the oceans?: *Earth and Planetary Science Letters*, v. 109, p. 507–515.
- Khain, V. E., and Sestavinsky, K. B., 1991, *Historical Geotectonics of the Paleozoic (in Russian)*: Moscow, Russia, Nedra, 398 p.
- Kominz, M. A., 1984, Oceanic ridge volumes and sea level change—an error analysis, in Schlee, J., editor, *Interregional Unconformities and Hydrocarbon Accumulation*: American Association of Petroleum Geologists Memoir 36, p. 109–127.
- Kossinna, E., 1933, Die Erdoberfläche, in Gutenberg, B., editor, *Handbuch der Geophysik, Aufbau der Erde*, v. 2: Berlin, Germany, Gebrüder Bornträger, p. 869–954.
- Landing, E., 1994, Precambrian-Cambrian boundary global stratotype ratified and a new perspective of Cambrian time: *Geology*, v. 22, p. 179–182.
- Larson, R. L., 1991, Latest pulse of the Earth: evidence for a mid-Cretaceous superplume: *Geology*, v. 19, p. 547–550.
- Levy, M., and Christie-Blick, N., 1991, Tectonic subsidence of the early Paleozoic passive continental margin in eastern California and southern Nevada: *Geological Society of America Bulletin*, v. 103, p. 1590–1606.
- McKerrow, W. S., Scotese, C. R., and Brasier, M. D., 1992, Early Cambrian continental reconstructions: *Journal of the Geological Society of London*, v. 149, p. 599–606.
- Miall, A. D., 1986, Eustatic sea level changes interpreted from seismic stratigraphy: a critique of the methodology with particular reference to the North Sea Jurassic record: *American Association of Petroleum Geologists Bulletin*, v. 70, p. 131–137.
- Mörner, N.-A., 1976, Eustasy and geoid changes: *Journal of Geology*, v. 84, p. 123–151.

- Nie, S.-Y., Rowley, D. B., and Ziegler, A. M., 1990, Constraints on the locations of Asian microcontinents in Palaeo-Tethys during the Late Palaeozoic, in McKerrow, W. S., and Scotese, C. R., editors, *Palaeozoic Palaeogeography and Biogeography: Geological Society of London Memoir 12*, p. 397–409.
- Palaeogeographic Atlas of Australia, 1988, v. 1—Cambrian: Canberra, Australian Government Publishing Service.
- 1992, v. 2—Ordovician: Canberra, Australian Government Publishing Service.
- Pitman, W. C., III, 1978, Relationship between eustasy and stratigraphic sequences of passive margins: *Geological Society of America Bulletin*, v. 89, p. 1389–1403.
- Railsback, L. B., 1992, A geological numerical model for Paleozoic global evaporite deposition: *Journal of Geology*, v. 100, p. 261–277.
- Riding, R., 1984, Sea-level changes and the evolution of benthic marine calcareous algae during the Palaeozoic: *Journal of the Geological Society of London*, v. 141, p. 547–553.
- Robardet, M., Paris, F., and Racheboeuf, P. R., 1990, Palaeogeographic evolution of southwestern Europe during Early Palaeozoic times, in McKerrow, W. S., and Scotese, C. R., editors, *Palaeozoic Palaeogeography and Biogeography: Geological Society of London Memoir 12*, p. 411–419.
- Ronov, A. B., 1994, Phanerozoic transgressions and regressions on the continents: a quantitative approach based on areas flooded by the sea and areas of marine and continental deposition: *American Journal of Science*, v. 294, p. 777–801.
- Ronov, A. B., Khain, V. E., Balukhovskiy, A. N., and Soslavinsky, K. B., 1980, Quantitative analysis of Phanerozoic sedimentation: *Sedimentary Geology*, v. 25, p. 311–325.
- Ronov, A. B., Khain, V. E., and Soslavinsky, K. B., 1976, The Ordovician lithologic association of the World: *International Geological Review*, v. 18, p. 1395–1412.
- 1984, *Atlas of Lithologic-Palaeogeographic Maps of the World—Late Precambrian and Palaeozoic of Continents* (in Russian and English): Leningrad, U.S.S.R. Academy of Sciences, 70 p.
- Ronov, A. B., Migdisov, A. A., and Khain, V. E., 1972, Quantitative methods of investigation in lithology and geochemistry (in Russian): *Litologia i Poleznye iskopaemiy*, No. 1, p. 3–14.
- Ross, C. A., and Ross, J. R. P., 1988, Late Paleozoic transgressive-regressive deposition, in Wilgus, C. K., and others, editors, *Sea-Level Change: An Integrated Approach*: Tulsa, Oklahoma, Society of Economic Paleontologists and Mineralogists, Special Publication 42, p. 227–247.
- Sahagian, D., 1987, Epeirogeny and eustatic sea level as inferred from Cretaceous shoreline deposits: applications to the central and western United States: *Journal of Geophysical Research*, v. 92, p. 4895–4904.
- 1988, Epeirogenic motions of Africa as inferred from Cretaceous shoreline deposits: *Tectonics*, v. 7, p. 125–138.
- Schubert, G., and Reymer, A. P. S., 1985, Continental volume and freeboard through geological time: *Nature*, v. 316, p. 336–339.
- Schuchert, C., 1955, *Atlas of Paleogeographic Maps of North America*: New York, Wiley, 177 p. + 84 maps.
- Scotese, C. R., Bambach, R. K., Barton, C., Van der Voo, R., and Ziegler, A. M., 1979, Paleozoic base maps: *Journal of Geology*, v. 87, p. 217–277.
- Scotese, C. R., and McKerrow, W. S., 1990, Revised World maps and introduction, in McKerrow, W. S., and Scotese, C. R., editors, *Palaeozoic Palaeogeography and Biogeography: Geological Society of London Memoir 12*, p. 1–21.
- Sempéré, J.-C., Palmer, J., Christie, D. M., Morgan, J. P., and Shor, A. N., 1991, Australian-Antarctic discordance: *Geology*, v. 19, p. 429–432.
- Soslavinsky, K. B., 1986, Tectonic evolution of the continents during Early and Middle Paleozoic time: *International Geological Review*, v. 28, p. 751–764.
- 1987, Sedimentation and volcanism during the Caledonian stage of Earth history (in Russian): Moscow, Russia, Nedra, 192 p.
- 1991, Global transgressions and regressions of the Paleozoic (in Russian): *Izvestia of the U.S.S.R. Academy of Sciences, Geological Series*, No. 1, p. 71–79; and *International Geological Review*, v. 33, p. 107–114.
- Sloss, L. L., 1963, Sequences in the cratonic interior of North America: *Geological Society of America Bulletin*, v. 74, p. 93–114.
- Smith, A. G., 1982, Late Cenozoic uplift of stable continents in a reference frame fixed to South America: *Nature*, v. 296, p. 400–404.
- Tardy, Y., N'Kounkou, R., and Probst, J.-L., 1989, The global water cycle and continental erosion during Phanerozoic time (570 my): *American Journal of Science*, v. 289, p. 455–483.

- Torsvik, T. H., Ryan, P. D., Trench, A., and Harper, D. A. T., 1991, Cambrian-Ordovician paleogeography of Baltica: *Geology*, v. 19, p. 7-10.
- Vail, P. R., Mitchum, R. M., Jr., and Thompson, S., III, 1977, Global cycles of relative changes of sea level, in Payton, C. E., editor, *Seismic Stratigraphy and Global Changes of Sea Level*: Tulsa, American Association of Petroleum Geologists Memoir 26, p. 83-97.
- Veevers, J. J., editor, 1984, *Phanerozoic Earth History of Australia*: Oxford, United Kingdom, Clarendon, 418 p.
- Vinogradov, A. P., editor, 1967-69, *Atlas of Lithologic-Paleogeographic Maps of the USSR* (4 vols., in Russian): Moscow, Russia, Ministry of Geology.
- Wang, H.-Z., compiler, 1985, *Atlas of the Palaeogeography of China*: Beijing, China, Cartographic Publishing House, 28 p. + 143 maps.
- Watts, A. B., and Steckler, M. S., 1979, Subsidence and eustasy at the continental margins of eastern North America, in Talwani, M., Hay, W., and Ryan, W. B. F., editors, *Deep Drilling Results in the Atlantic Ocean: Continental Margins and Paleoenvironment*: Washington, D. C., American Geophysical Union Maurice Ewing Series 3, p. 218-234.
- Wilkinson, B. H., and Given, R. K., 1986, Secular variation in abiotic marine carbonates: Constraints on Phanerozoic atmospheric carbon dioxide contents and oceanic Mg/Ca ratios: *Journal of Geology*, v. 94, p. 321-333.
- Wilkinson, B. H., Owen, R. M., and Carroll, A. R., 1985, Submarine hydrothermal weathering, global eustasy, and carbonate polymorphism in Phanerozoic marine oolites: *Journal of Sedimentary Petrology*, v. 55, p. 171-183.
- Wilkinson, B. H., and Walker, J. C. G., 1989, Phanerozoic cycling of sedimentary carbonate: *American Journal of Science*, v. 289, p. 525-548.
- Wise, D. U., 1974, Continental margins, freeboard and the volumes of continents and oceans through time, in Burk, C. A., and Drake, C. L., editors, *The Geology of Continental Margins*: New York, Springer, p. 45-58.
- Worsley, T. R., Nance, D., and Moody, J. B., 1984, Global tectonics and eustasy for the past 2 billion years: *Marine Geology*, v. 58, p. 373-400.
- Wyatt, A. R., 1984, Relationships between continental area and elevation: *Nature*, v. 311, p. 370-372.
- Ziegler, P. A., 1989, *Evolution of Laurussia*: Dordrecht, Kluwer, 102 p.
- Zonenshain, L. P., Kuzmin, M. I., and Kononov, M. V., 1987, Absolute reconstructions of the state of continents in Paleozoic and Early Mesozoic: *Geotectonics*, v. 21, p. 199-212.
- Zonenshain, L. P., Kuzmin, M. I., and Natapov, L. M., 1990, *Geology of the USSR: A Plate-Tectonic Synthesis* (Page, B. M., editor), *Geodynamics Series 21*: Washington, D.C., American Geophysical Union, 242 p.